

1 **Polygenic adaptation and negative selection across traits, years and environments in a
2 long-lived plant species (*Pinus pinaster* Ait., Pinaceae)**

3 Marina de Miguel[†], Isabel Rodríguez-Quilón[‡], Myriam Heuertz[†], Agathe Hurel[†], Delphine
4 Grivet[‡], Juan-Pablo Jaramillo-Correa^{*}, Giovanni G. Vendramin[§], Christophe Plomion[†], Juan
5 Majada^{††}, Ricardo Alía[‡], Andrew J. Eckert^{‡‡}, Santiago C. González-Martínez^{†§§}

6 [†]INRAE, Univ. Bordeaux, BIOGECO, F-33610 Cestas, France

7 [‡]Department of Forest Ecology and Genetics, Forest Research Centre, INIA, Carretera de la
8 Coruña km 7.5, 28040 Madrid, Spain

9 ^{*}Department of Evolutionary Ecology, Institute of Ecology, Universidad Nacional Autónoma
10 de México, AP 70-275 México City, CDMX 04510, Mexico

11 [§]Institute of Biosciences and Bioresources, Division of Florence, National Research Council,
12 50019 Sesto Fiorentino (FI), Italy

13 ^{††}Sección Forestal, SERIDA, Finca Experimental “La Mata”, 33820 Grado, Principado de
14 Asturias, Spain

15 ^{‡‡}Department of Biology, Virginia Commonwealth University, Richmond, VA 23284, USA

16

17 ^{§§}Corresponding author

18

19 **Running title:** Polygenic adaptation in maritime pine

20

21 **Keywords:** heritability, local adaptation, maritime pine, polygenicity, natural selection

22

23 Corresponding author:

24 Santiago C. González-Martínez

25 UMR 1202 INRAE – Univ. Bordeaux

26 69 route d’Arcachon, F-33610 Cestas, France

27 Tel: +33 (0) 5 35 38 53 20

28 santiago.gonzalez-martinez@inrae.fr

29

30 **Abstract**

31 A decade of association studies in multiple organisms suggests that most complex traits are
32 polygenic; that is, they have a genetic architecture determined by numerous loci distributed
33 across the genome, each with small effect-size. Thus, determining the degree of polygenicity
34 and its variation across traits, environments and years is useful to understand the genetic basis
35 of phenotypic variation. In this study, we applied multilocus approaches to estimate the
36 degree of polygenicity of fitness-related traits in a long-lived plant (*Pinus pinaster* Ait.,
37 maritime pine) and to analyze how polygenicity changes across environments and years. To
38 do so, we evaluated five categories of fitness-related traits (survival, height, phenology-
39 related, functional, and biotic-stress response traits) in a clonal common garden network,
40 planted in contrasted environments (over 12,500 trees). First, most of the analyzed traits
41 showed evidence of local adaptation based on Q_{ST} - F_{ST} comparisons. Second, we observed a
42 remarkably stable degree of polygenicity, averaging 6% (range of 0-27%), across traits,
43 environments and years. As previously suggested for humans, some of these traits showed
44 also evidence of negative selection, which could explain, at least partially, the high degree of
45 polygenicity. The observed genetic architecture of fitness-related traits in maritime pine
46 supports the polygenic adaptation model. Because polygenic adaptation can occur rapidly, our
47 study suggests that current predictions on the capacity of natural forest tree populations to
48 adapt to new environments should be revised, which is of special relevance in the current
49 context of climate change.

50

51

52

53 **Introduction**

54 Population adaptive responses to environmental changes depend on the genetic architecture of
55 fitness-related traits (Hayward and Sella 2019). Although not initially conceived for the study
56 of adaptation, genome-wide association studies (GWAS) have provided essential information
57 to understand the genetic basis of complex traits. The implementation of GWAS allowed the
58 identification of genetic variants affecting fitness-related traits, their allele frequencies, the
59 magnitudes of their effects, and their interactions with one another and the environment.
60 Examples exist for humans (reviewed by Visscher *et al.* 2017), other animals (e.g. Sharma *et*
61 *al.* 2015; Pitchers *et al.* 2019) and plants (e.g. González-Martínez *et al.* 2006; Huang and Han
62 2014; Alonso-Blanco *et al.* 2016). Surprisingly, in some species, such as humans and forest
63 trees (Resende *et al.* 2012; Lind *et al.* 2018), the genetic variants associated with phenotypic
64 variation accounted for only small fractions of trait heritability, as estimated through pedigree
65 analysis, causing the so-called ‘missing heritability’ paradox (Maher 2008). Several
66 explanations have been provided to solve this paradox (Manolio *et al.* 2009; Brachi *et al.*
67 2011; Björkegren *et al.* 2015; Pallares 2019). In particular, different sources of evidence point
68 to polygenicity, i.e. trait architecture determined by a large number of variants, each with a
69 small effect-size, as a potential reason for the low levels of heritability explained by current
70 GWAS, which would thus be unpowered to detect most causal variants (Yang *et al.* 2010; Shi
71 *et al.* 2016; Boyle *et al.* 2017).

72 The study of adaptation has traditionally been addressed from contrasting research paradigms
73 (Höllinger *et al.* 2019). While quantitative genetic approaches view adaptation as the result of
74 changes in allele frequencies at an idealized infinite number of loci, each with infinitesimal
75 effects on fitness (Fisher 1918), population genetic approaches made more emphasis in the
76 detection of selective sweeps, where new beneficial mutations rapidly become fixed at a small
77 number of loci (Smith and Haigh 1974). The hypothesis that natural selection (mostly) acts

78 through subtle allele frequency shifts on standing genetic variation at numerous loci
79 distributed across the genome has been suggested in previous evolutionary studies (Orr and
80 Coyne 1992; e.g. McKay and Latta 2002; Le Corre and Kremer 2003). Nevertheless, it was
81 Pritchard *et al.* (2010) who first brought together population and quantitative genetic theory
82 with conclusions from GWAS to formulate a new model for the study of adaptation – the
83 polygenic adaptation model. Under this model, some genes may harbor new mutations that
84 have been fixed by natural selection, but the most common pattern would be the genome-wide
85 increase of favored alleles, without the fixation of most causative variants. Thus, the expected
86 genome-wide footprint resulting from natural selection would not be that of a classical hard
87 sweep, but would rather involve a large number of causal variants, each with subtle allele
88 frequency changes (Pritchard *et al.* 2010; Pritchard and Rienzo 2010; Hermisson and
89 Pennings 2017).

90 Several new methods have been developed to detect the genetic signatures of natural selection
91 under the polygenic adaptation model (Guan and Stephens 2011; Turchin *et al.* 2012; Daub *et*
92 *al.* 2013; Berg and Coop 2014; Field *et al.* 2016; Zeng *et al.* 2018; Edge and Coop 2019;
93 Speidel *et al.* 2019; Lloyd-Jones *et al.* 2019). Applications using these methods, however,
94 were often unknowingly biased by subtle patterns of population structure (Liu *et al.* 2018;
95 Josephs *et al.* 2019; Rosenberg *et al.* 2019; Berg *et al.* 2019a; Sohail *et al.* 2019).
96 Nonetheless, even considering the inflation of polygenic signals due to unrecognized
97 population structure, mounting evidence over the last decade using a variety of
98 methodologies, supports the polygenic adaptation model in a diversity of organisms, such as
99 humans (Hancock *et al.* 2010a, b; Daub *et al.* 2013; Shi *et al.* 2016; Zeng *et al.* 2018;
100 Gnechi-Ruscone *et al.* 2018; Berg *et al.* 2019b), insects (Friedline *et al.* 2019), molluscs
101 (Bernatchez *et al.* 2019), model plants (He *et al.* 2016), crops (Josephs *et al.* 2019; Wisser *et*
102 *al.* 2019), and forest trees (Lind *et al.* 2017; De La Torre *et al.* 2019). However, there are still

103 multiple open questions regarding the degree of polygenicity at adaptive traits, the distribution
104 of effect sizes the involved loci, and how the genetic architecture changes under varying
105 selective forces, especially for non-model species (Lind *et al.* 2018).

106 Following the expectations of the polygenic adaptation model, the heritability of complex
107 traits is often associated with loci that are widespread across the whole genome, also
108 including SNPs located in genes and pathways that do not show a clear functional connection
109 to the trait of interest (Boyle *et al.* 2017). The omnigenic model, formulated by Boyle *et al.*
110 (2017), provides a plausible hypothesis to explain this. The interconnection of gene regulatory
111 networks implies that the vast majority of expressed genes likely influence the functions of
112 core genes directly linked to fitness-related traits. Nevertheless, the study of polygenic
113 adaptation at the pathway level is useful to identify gene sets of special relevance for
114 adaptation (Daub *et al.* 2013). In particular, polygenic adaptation at pathway level has been
115 proved especially useful to study non-model species, as reliance on selective sweep models
116 often led to poor inferences (Hämälä *et al.* 2020). For example, Mayol *et al.* (2020) detected
117 signatures of polygenic selection at the pathway level in English yew (*Taxus baccata* L.)
118 *Taxus baccata* and identified negative selection as an important mechanism driving the
119 pathway-level signal. Similarly, negative selection has been identified as a pervasive
120 mechanism determining the polygenic architecture of fitness-related traits in humans (Zeng *et*
121 *al.* 2018; O'Connor *et al.* 2019). In particular, negative selection has been proposed to favor
122 polygenicity in complex traits by removing large-effect variants, because of their deleterious
123 effects, while small-effect variants would remain unaffected; a process named ‘flattening’, as
124 the genetic signal is ‘flattened’ relative to the underlying biology (O'Connor *et al.* 2019).

125 Despite theoretical advances and the development of new methods to study polygenic
126 adaptation, the addressed questions remain constrained by the specific life-history traits of a
127 few model species. Maritime pine (*Pinus pinaster* Ait.) is an ideal case study to investigate

128 polygenic adaptation in an ecologically and economically important group of species, the
129 forest trees: it is a long-lived plant inhabiting nearly undomesticated random-mating
130 populations with high genetic diversity (González-Martínez *et al.* 2002; Jaramillo-Correa *et*
131 *al.* 2015). It expanded from several isolated glacial refugia, and it is now distributed across
132 the western Mediterranean Basin and the European Atlantic front in scattered populations
133 under contrasting environments (Bucci *et al.* 2007). In addition, an artificial clonal
134 propagation program in maritime pine allowed us to estimate precisely variance components
135 and investigate selective forces driving trait evolution under contrasting environments.
136 Specifically, we i) tested the hypothesis that most complex adaptive traits in a long-lived plant
137 are polygenic, providing a first estimate of the degree polygenicity in a forest tree, and ii) that
138 their genetic architecture is mostly driven by negative selection. We then iii) investigated how
139 these patterns change with time and through environmental settings, which is of special
140 relevance for long-lived organisms, such as forest trees.

141 **Materials and Methods**

142 *Clonal common garden network (CLONAPIN)*

143 We studied phenotypic variation in a clonal common garden network (CLONAPIN)
144 composed of five sites covering the natural environmental range of maritime pine, from harsh
145 Mediterranean climates to mild Atlantic ones. Common gardens comprise trees from 36
146 populations, sampled across the species natural distribution and covering the six previously
147 identified gene pools for this species (Jaramillo-Correa *et al.* 2015; Supplemental Figure S1).
148 Open-pollinated seeds were collected in natural stands, and germinated in a nursery; then one
149 seedling per open-pollinated family was selected and vegetatively propagated by cuttings
150 (following Majada *et al.* 2011). A total of 535 genotypes (clones) belonging to 35 populations
151 were used to establish four of the clonal common gardens (three sites in Spain: Cabada,

152 Cáceres and Madrid; and one in Portugal: Fundão; Table 1) with eight ramets per clone set in
153 a randomized complete block design ($N=4,273$ trees). These clonal common gardens were
154 planted in 2010. In 2011, a fifth common garden was established in Pierroton (France),
155 comprising 443 clones from all 36 populations ($N=3,434$ trees). Common gardens in Cabada,
156 Fundão and Pierroton are located in the Atlantic region, with high annual rainfall and mild
157 temperatures. Common gardens in Cáceres and Madrid are located in continental areas under
158 Mediterranean influence, with large seasonal temperature oscillations and a marked summer
159 drought. In addition, clay soils in Cáceres hampered plant growth and diminished survival
160 (Table 1).

161 *Phenotypic evaluation*

162 A total of 28 phenotypic trait-environment combinations were evaluated in this study.
163 Assayed phenotypic traits were classified into five groups: survival, height, phenology-
164 related, functional, and biotic-stress response (see Supplemental Table S1 for an exhaustive
165 list of the measured traits). In brief, tree survival and height were evaluated in the five
166 common gardens (including different years in Pierroton, with measures taken in 2013, 2015,
167 and 2018). Phenology-related traits were evaluated in the Atlantic sites only (Cabada, Fundão
168 and Pierroton), including different years of evaluation in Pierroton (2015 and 2017). In
169 Cabada and Fundão, growth phenology was estimated through the presence of polycyclism
170 (i.e. the ability for a plant to produce several flushes in the same growing season; (Girard *et*
171 *al.* 2011)) and a phenology growth index (1):

$$172 \text{ Phenology Growth Index} = \frac{\text{spring growth}}{\text{total growth}} = \frac{(\text{tree height } \textit{may}_n - \text{tree height } \textit{dec}_{n-1})}{(\text{tree height } \textit{dec}_n - \text{tree height } \textit{dec}_{n-1})} \quad (1)$$

173 where *may* and *dec* correspond to the months May and December of the year n and the year n-
174 1, respectively.

175 In Pierrotin, phenology of bud burst was estimated through a scale ranging from 0 to 5 (0:
176 bud with no winter elongation, 1: elongation of the bud, 2: emergence of brachyblasts, 3:
177 brachyblasts begin to separate, 4: elongating needles, 5: total elongation of the needles) (see
178 Hurel *et al.* 2019). The first Julian day at each stage (S1 to S5) was scored for each tree.
179 Julian days were converted into accumulated degree-days (with base temperature 0°C) from
180 the first day of the year, to take into account the between-year variability in temperature. The
181 number of degree-days between stages 1 and 4 defines the duration of bud burst. Daily mean
182 temperatures to calculate accumulated degree-days were downloaded from the nearest
183 climatic station (located just a few hundred meters from the common garden, station
184 33122004 of the INRAE Agroclim database: <https://www6.paca.inrae.fr/agroclim/Les-outils>).

185 Functional traits, including nitrogen and carbon content and isotopic composition ($\delta^{15}\text{N}$ and
186 $\delta^{13}\text{C}$, respectively), as well as specific leaf area (SLA, a measure of leaf area per unit of dry
187 mass), were evaluated in the common garden located in Fundão (Portugal). A bulk of five
188 needles positioned 10 cm below the upper part of the shoot to avoid sampling bias (Warren *et*
189 *al.* 2001) were sampled and prepared in a standard way for analysis (Brendel 2001).
190 Determination of carbon content and isotopic composition was performed with a mass
191 spectrometer at the University of Colorado isotope laboratory. Raw values were corrected by
192 their position in the plate according to the standards, and this value was used for the
193 subsequent analysis. SLA is an estimation of the compromise among light capture, CO_2
194 assimilation, and the restrictions imposed by water loss through transpiration (Sefton *et al.*
195 2002). Low SLA suggests high leaf construction cost, and thus higher stress tolerance (Díaz *et*
196 *al.* 2016). Thus, this key leaf trait is also associated with fitness components, such as tree
197 survival (Greenwood *et al.* 2017). Given that there is a positive relationship between $\delta^{13}\text{C}$ and
198 water use efficiency (Farquhar and Richards 1984), $\delta^{13}\text{C}$ has been widely used as a surrogate
199 to study tree adaptation to water-limiting environments (e.g. Aranda *et al.* 2010; Walker *et al.*

200 2015). Similarly, $\delta^{15}\text{N}$ is an indirect index related to the nitrogen cycle (Craine *et al.* 2015).

201 Assessment of biotic-stress response in a high number of trees is logistically complex.
202 Therefore, it was evaluated only for a subset of clones (see Supplemental Table S1) in the
203 Pierrotot common garden (France). This common garden was selected because of the
204 importance of the Landes region in maritime pine breeding for wood production. Biotic-stress
205 response was evaluated based on susceptibility to two major pine pathogens, *Diplodia sapinea*
206 and *Armillaria ostoyae*, as well as the incidence of the defoliator pest, *Thaumetopoea*
207 *pityocampa* (pine processionary moth) (see Hurel *et al.* 2019 for details). *D. sapinea* causes
208 several diseases in conifers, which may be exacerbated under climate change and compromise
209 pine forest health (Desprez-Loustau *et al.* 2006). Susceptibility to *D. sapinea* was evaluated
210 following controlled inoculation as the lesion extent around the inoculated site (hereafter
211 referred as necrosis) and a scalar notation of needle discoloration (0: no discoloration, 2: some
212 needles around the necrosis were discolored, and 3: all needles around the necrosis were
213 discolored). *A. ostoyae* is a conifer root pathogen causing growth cessation and eventually
214 death (Heinzelmann *et al.* 2019). To evaluate the incidence of this pathogen, *A. ostoyae*
215 mycelium culture was prepared in plastic jars. The level of humidity observed in the plastic
216 jar was visually scored as dry, medium or humid. Susceptibility to *A. ostoyae* was assessed
217 after controlled inoculation as the lesion length in the sapwood (i.e. wood browning, hereafter
218 also referred as necrosis). We accounted for the potential influence of variation in humidity on
219 wood browning by including the level of humidity in the jar as a covariate for *A. ostoyae*
220 susceptibility analysis (see below). Finally, the pine processionary moth is an insect that
221 rapidly defoliates pines leading to forest decline (Jacquet *et al.* 2013). The presence or
222 absence of pine processionary moth nests in the tree crowns was assessed in March 2018.

223 *DNA extraction and SNP genotyping*

224 Needles were collected from one ramet per clone in the Cabada common garden ($N=523$).
225 Genomic DNA was extracted using the Invisorb® DNA Plant HTS 96 Kit/C kit (Invitek
226 GmbH, Berlin, Germany). A 9k *Illumina Infinium* SNP array developed by Plomion *et al.*
227 (2016b) was used for genotyping. This array was constructed using previously identified and
228 newly *in silico*-developed SNPs, either from randomly screened EST sequences or
229 specifically detected at candidate genes for adaptation to biotic and abiotic factors (see
230 Plomion *et al.* 2016b for further details). Genotyped SNPs covered all 12 chromosomes of *P.*
231 *pinaster* according to previous linkage mapping (Plomion *et al.* 2016b). For this study, 6,100
232 SNPs were finally retained following standard filtering (GenTrain score > 0.35 , GenCall50
233 score > 0.15 and Call frequency > 0.85) and removal of SNPs with uncertain clustering
234 patterns (visual inspection using *GenomeStudio v. 2.0*). Individuals with more than 15%
235 missing data were also removed. This resulted in 5,165 polymorphic SNPs that were included
236 in the estimation of molecular population differentiation (F_{ST}) and the polygenic association
237 study.

238 *Quantitative genetics analysis*

239 Genetic components of the phenotypic variance were estimated using Generalized Linear
240 Mixed-Effects Models (GLMM) fitted in a Bayesian framework using Markov chain Monte
241 Carlo (MCMC) methods. The model, described in equation (2), was implemented for those
242 phenotypic traits evaluated at multiple sites of the CLONAPIN common garden network (see
243 Supplemental Table S1). To estimate the genetic control of the genotype-by-environment
244 (G×E) interactions, the model described in equation (3) was fitted for those traits measured at
245 all sites of the CLONAPIN common garden network (i.e. height and survival).

246
$$y_{ijkl} = \mu + S_i + S(B)_{ij} + P_k + P(C)_{kl} + S_i * C_l + \varepsilon_{ijkl} \quad (2)$$

247
$$y_{ijkl} = \mu + S_i + S(B)_{ij} + P_k + P(C)_{kl} + S_i * P_k + S_i * C_l + \varepsilon_{ijkl} \quad (3)$$

248 where, for a given trait y , μ denotes the overall phenotypic mean, S_i refers to the fixed effect
249 of site i , B_j represents the random effect of experimental block j nested within site i , P_k is the
250 random effect of population k , C denotes the random effect of clone l nested within
251 population k , and ε is the residual effect.

252 Simplified models with or without covariates represented by equations (4) and (5) were
253 implemented for phenotypic traits measured in just one site of the CLONAPIN common
254 garden network (see Supplemental Table S1).

255
$$y_{ijk} = \mu + B_i + P_j + P(C)_{jk} + \varepsilon_{ijk} \quad (4)$$

256
$$y_{ijk} = \mu + B_i + cov + P_j + P(C)_{jk} + \varepsilon_{ijk} \quad (5)$$

257 Where, for a given trait y , μ denotes the overall phenotypic mean, B_i represents the fixed
258 effect of experimental block i , P_j is the random effect of population j , C denotes the random
259 effect of clone k nested within population j , and ε is the residual effect. In the model
260 represented by equation (5), cov represents a covariate implemented when modeling the
261 presence of pine processionary moth nests (i.e. an estimate of tree height) and necrosis caused
262 by *A. ostoyae* (i.e., level of humidity in the experimental jar).

263 All models were fitted with the R package *MCMCglmm* (Hadfield 2010). Phenotypic traits
264 showing Gaussian distributions were modeled using the identity link function, while
265 phenotypic traits exhibiting a binomial distribution (survival, polycyclism, *D. sapinea* needle
266 discoloration, and presence or absence of pine processionary moth) were modeled either with
267 *logit* or *probit* link functions (see Supplemental Table S2 for an exhaustive list of model
268 parameter specifications). Multivariate-normal prior distributions with mean centered at zero
269 and large variance matrices (10^8) were used for fixed effects. For ordinal traits, a Gelman

270 prior for the variance of fixed effects was set, as suggested by Gelman *et al.* (2008). Inverse
271 Wishart non-informative priors were used for the variances and covariances of random
272 effects, with the matrix parameter V set to 1, and a parameter n set to 0.002 (Hadfield 2010).
273 Parameter expanded priors were used to improve the chain convergence and mixing, as
274 suggested by Gelman (2006) for models with near-zero variance components. Priors with a
275 larger degree of belief parameter (n set to 1), specifying that a large proportion of the
276 variation is under genetic control (as suggested by Wilson *et al.* 2010) did not change the
277 results (data not shown). Models were run for at least 550,000 iterations, including a burn-in
278 of 50,000 iterations and a thinning interval of 100 iterations. Four chains per model were run
279 to test for parameter convergence. The potential scale reduction factor (psrf) was consistently
280 below 1.02 for all the models (Supplemental Table S2) (Gelman and Rubin 1992).

281 Variance components were then used to compute broad-sense heritability (H^2) as (6):

$$282 \quad H^2 = \frac{\sigma_{clone}^2}{(\sigma_{clone}^2 + \sigma_e^2)} \quad (6)$$

283 where σ_{clone}^2 is the variance among clones within populations and σ_e^2 the residual variance.
284 For estimating broad-sense heritability for traits following a binomial distribution, we
285 included an extra term in the denominator ($+\pi^2/3$) to account for implicit *logit* link function
286 variance; similarly, we added one to the denominator to account for the *probit* link function
287 (Nakagawa and Schielzeth 2010).

288 The GLMMs described above were used to estimate genetic values using Best Linear
289 Unbiased Predictors (BLUPs) (Henderson 1973; Robinson 1991). The genetic value of each
290 clone was defined as the population BLUP plus the clone BLUP. BLUPs for GxE, were
291 obtained from equation (3) and calculated following equation (7).

$$292 \quad G \times E BLUP = \left(\frac{\sum BLUP_{pop\ atl}}{N\ atl} - \frac{\sum BLUP_{pop\ med}}{N\ med} \right) + \left(\frac{\sum BLUP_{clone\ atl}}{N\ atl} - \frac{\sum BLUP_{clone\ med}}{N\ med} \right) \quad (7)$$

293 where $BLUP_{pop\ atl}$ is the population BLUP in sites under Atlantic climate (Cabada, Fundão,
294 and Pierrotón), $BLUP_{pop\ med}$ the population BLUP in sites under Mediterranean climate
295 (Cáceres and Madrid), $BLUP_{clone\ atl}$ the clone BLUP in sites under Atlantic climate,
296 $BLUP_{clone\ med}$, the clone BLUP in sites under Mediterranean climate, $N\ atl$ the number of
297 sites under Atlantic climate, and $N\ med$ the number of sites under Mediterranean climate.

298 Parameter estimates from quantitative genetics analyses are presented as the mode of the
299 posterior distribution; 95% credible intervals were computed as the highest density region of
300 each posterior parameter distribution.

301 *Q_{ST}-F_{ST} comparison*

302 Molecular population differentiation (F_{ST}) was estimated according to Weir and Cockerham
303 (1984) using the 5,165 SNPs from the *Illumina Infinium* SNP array and the diveRsity R
304 package (Keenan *et al.* 2013). The 95% confidence interval of the global F_{ST} estimate was
305 computed by bootstrapping across loci (1,000 bootstrap iterations). Quantitative genetic
306 differentiation among populations was calculated following Spitze (1993) using the variance
307 components estimated from the previously described models (equations 2-5):

308
$$Q_{ST} = \frac{\sigma_{pop}^2}{\sigma_{pop}^2 + 2\sigma_{clone}^2} \quad (8)$$

309 where σ_{pop}^2 is the variance among populations, and σ_{clone}^2 is the variance among clones within
310 populations. Quantitative (Q_{ST}) and molecular (F_{ST}) genetic differentiation among populations
311 were considered significantly different when Q_{ST} and F_{ST} posterior distributions had non-
312 overlapping 95% confidence intervals.

313 *Polygenicity across traits, years and environments*

314 Polygenicity was evaluated as the proportion of SNPs with non-zero effects on phenotypic

315 traits. First, we conducted posterior inference via model averaging and subset selection
316 (VSR), as implemented in piMASS software (Guan and Stephens 2011). This method allows
317 to identify combinations of SNPs likely affecting a phenotype and to estimate the proportion
318 of trait variance explained by the SNPs in the data set. Hereafter, we referred to this quantity
319 as the genetic explained variance (*GEV*), which, in this study, represents the BLUP variance
320 explained by SNP additive effects. Second, we used the Bayesian mixed linear model (MLM)
321 framework developed by Zeng *et al.* (2018) as implemented in CGTB 2.0 software. This last
322 model simultaneously estimates: i) SNP-based heritability (considering the SNPs with non-
323 zero effects on the trait), hereafter referred as *GEV*, analogously to VSR estimates, ii)
324 polygenicity (as defined above), and iii) the relationship between SNP effect-size and minor
325 allele frequency (*S*, a common indicative of negative selection). When negative selection is
326 operating, *S* is expected to be negative, as most new mutations are deleterious and high-effect
327 SNPs are kept at low frequencies. Estimates with 95% credible intervals of parameter
328 posterior distributions not overlapping zero were considered as significant. Prior to these
329 analyses, neutral population genetic structure was accounted for by running linear models
330 relating the genetic values for each trait (with site and block effects removed) to the admixture
331 coefficients for each clone (*Q*-scores) obtained using a STRUCTURE run for *K*=6 based on
332 neutral markers (see Jaramillo-Correa *et al.* 2015 for further details). From this linear model,
333 we extracted the normalized residuals for each trait, as recommended in piMASS manual.

334 Analyses were run separately for different traits, years, and environments (see Supplemental
335 Table S1). VSR models were run for 2,000,000 iterations with a burn-in of 100,000 iterations
336 and a thinning interval of 100. After several preliminary runs, the maximum number of SNPs
337 included in VSR models was fixed to 2,000 (i.e. maximum allowed polygenicity of ~40%).
338 MLM models were run for 500,100 iterations, including a burn-in of 100 iterations, and a
339 thinning interval of 10 iterations. Parameter estimates from both VSRs and MLMs were

340 presented as the median of the posterior distribution, instead of the mode, for better handling
341 of bimodal distributions (Supplemental Figure S2). The 95% credible intervals were
342 computed as the highest density region of the posterior parameter distribution, as above.

343 *Annotation and gene function enrichment at pathway level*

344 The transcripts containing the 5,165 polymorphic SNPs were downloaded from SustainPine
345 v.3.0 database (Canales *et al.* 2014). DNA sequences were translated with BioEdit v. 7.2.6
346 (Hall 1999) and submitted to BlastKOALA (Kanehisa *et al.* 2016) for annotation and
347 functional characterization using InterPro annotations, GO terms, and KEGG pathway
348 identification. Annotations were compared with those available at SustainPine, and
349 conflicting cases were examined individually by privileging similarity to genes correctly
350 identified in other conifers or forest trees. Contigs with no clear annotations (e.g. hypothetical
351 or unknown proteins, or unsolved conflicting annotations) were removed from the database.
352 For the retained contigs, the top-two KEGG terms were used for assignation to one or more
353 specific metabolic pathways/modules based on KEGG orthology. Genes for which no hit with
354 KEGG database was found, were assigned to metabolic pathways/modules based on the
355 InterPro annotation. We privileged metabolic pathways/modules that could be unequivocally
356 assigned to a given phenotypic response (e.g. circadian rhythm to bud phenology or pathogen
357 interaction to biotic stress response) or linked to various stress responses (e.g. DNA
358 recombination and repair, ubiquitin system or transcription factor machinery to survival and
359 biotic stress response). In total, seventeen pathways/modules were retained containing a total
360 of 628 (19.7% out of 3,194) genes, with 1,233 polymorphic SNPs (Supplemental Table S3).

361 For enrichment tests using polysel (Daub *et al.* 2013), the seventeen pathways/modules were
362 defined as gene sets. First, we computed two statistics at the gene level (i.e. objStat in polysel)
363 based on the per-SNP estimates obtained from the VSR implemented in piMASS: the

364 maximum, over all SNPs included in a gene, of the Rao-Backwellized posterior probability of
365 inclusion *maxpostrb*, and the maximum of the absolute value of Rao-Backwellized effect size
366 *maxabsbetarb*. To account for a weak correlation of these statistics with the number of SNPs
367 per gene, we used the AssignBins and RescaleBins functions in polysel, which automatically
368 assigns gene scores (objStat) into bins defined from the number of SNPs per gene. We then
369 rescaled scores within bins and computed the sum(objStat) of each statistic over all genes per
370 gene set. Since the sum(objStat) for random gene sets (sizes n = 10, 50, 250 genes) was not
371 normally distributed, we built empirical null distributions by randomly sampling gene sets of
372 the same size as the sets to be tested. Then, we performed one-sided tests evaluating whether
373 the observed sum(objStat) was smaller than the 5th or larger than the 95th percentile of the
374 sum(objStat) null distribution. Higher-tail significant results for *maxpostrb* indicate gene sets
375 enriched with higher overall probability of being selected during the VSR procedure
376 implemented in piMASS. Higher-tail significant results for *maxabsbetarb* points to gene sets
377 enriched with higher overall SNP effect-sizes. Contrarily, lower-tail significant results for
378 both statistics suggests conserved gene sets, containing genes with smaller overall probability
379 of inclusion or SNP effect-size estimates. We report *p*-values based on this comparison, as
380 well as *q*-values from a False Discovery Rate (FDR) approach implemented in the R package
381 *qvalue* (R Core Team 2019). The level of connection between gene sets was weak with only
382 four genes associated with more than one gene set (633 gene – gene set combinations for 628
383 genes). For this reason, we did not assess enrichment for pruned gene sets (see Daub *et al.*
384 2013).

385 **Results**

386 *Broad-sense heritability and genetic differentiation among populations*

387 All traits had low to moderate estimates of broad-sense heritability (Supplemental Table S1),
388 with the exception of nitrogen and carbon amount that did not show genetic variation.
389 Consequently, polygenic association methods failed to converge for these two traits and they
390 were excluded from further analyses. H^2 ranged from 0.32 for bud burst measured in 2015 to
391 zero for survival in the French Atlantic environment in 2013. Interestingly, survival showed
392 significant estimates of H^2 only in the sites under (harsher) Mediterranean climate. The
393 highest H^2 estimates were observed for phenology-related traits followed by tree height. H^2 for
394 a given trait varied across environments (e.g. height, survival and phenology-related traits) but
395 showed little variation across years (Supplemental Table S1).

396 The global F_{ST} was 0.112 (95% confidence interval: 0.090 - 0.141). All groups of phenotypic
397 traits, excepting survival, had at least one trait with statistically higher Q_{ST} than F_{ST}
398 (Supplemental Table S1). The highest Q_{ST} was obtained for susceptibility to *D. sapinea*
399 infection measured as necrosis length, followed by $\delta^{13}\text{C}$ and tree height, which also showed
400 similar Q_{ST} values across environments and tree ages (Figure 1).

401 *Genetic architecture (polygenicity) of adaptive traits*

402 Polygenicity estimates were consistent between the VSR and MLM methods (Supplemental
403 Table S4). Both methods showed substantial polygenic control for most of the phenotypic
404 traits, with an average of 6% (0-27%) of the genotyped SNPs having non-zero effects.
405 Significant polygenicity was found in all five trait categories for at least one trait (Figures 2
406 and 3; Supplemental Table S4). Polygenicity for height was stable across environments and
407 years, when measured multiple times under the same environment (i.e. in the French Atlantic
408 common garden) (Figure 3). Along the same line, polygenicity for phenology-related traits
409 and tree survival also remained stable across environments, although 95% credible intervals
410 overlapped zero in some cases. The low polygenicity values observed for survival in the

411 French Atlantic common garden are probably a consequence of the low levels of phenotypic
412 variability in this site, with almost no mortality (97.12% of planted trees were alive at the
413 evaluation time, Supplemental Table S1). Polygenicity was heterogeneous for biotic-stress
414 response and functional traits (Figure 2). For instance, susceptibility to *D. sapinea* was more
415 polygenic than to *A. ostoyae* or than incidence of pine processionary moth. For functional
416 traits, SLA and $\delta^{15}\text{N}$ showed the highest levels of polygenicity, while $\delta^{13}\text{C}$ showed a
417 considerably lower proportion of SNPs with non-zero effects.

418 In addition, *GEV* was consistent between methods, although VSR tended to render higher
419 values (Supplemental Table S4). On average *GEV* was 0.38 across traits, with a minimum of
420 0.018 for survival in the French Atlantic environment in 2018, and a maximum of 0.99 for *D.*
421 *sapinea* necrosis. *GEV* estimated with the VSR method for the G×E component on tree height
422 (considering Atlantic versus Mediterranean environments) was low but significant (median =
423 0.238, 95% credible interval = 0.043 - 0.409), indicating some SNPs with significant effects
424 on growth plasticity. However, this result could not be confirmed with the MLM method.
425 Moreover, *GEV* for the G×E component on tree survival was not significant with any model.

426 Polygenicity and *GEV* were positively and consistently correlated for both VSR and MLM
427 models (Figure 4). This positive correlation suggested that SNP-based heritability is mainly
428 determined by genetic variants with similarly small effects, and that differences in
429 polygenicity across traits are mostly accounting for differences in explained genetic variance,
430 rather than the distribution of SNP effect-size (Supplemental Figures S2 and S3).

431 *Evidence of negative selection*

432 The correlation between SNP effect-size and minor allele frequency (MAF), *S*, was used to
433 identify the type and mode of natural selection acting upon phenotypic traits. Out of the 28
434 assayed traits, we were able to estimate *S* through the MLM method for 19 of them. Estimates

435 ranged from -1.68 (bud burst in 2017) to 0.55 (tree survival in French Atlantic environment),
436 but only seven traits from four out of five trait categories (survival, height, phenology-related,
437 and functional traits) were significant (Figure 5). No significant effect was observed for any
438 trait belonging to the biotic-stress response category. Remarkably, all seven significant
439 estimates of S were negative (ranging from -1.68 for bud burst in 2017 to -0.99 for survival in
440 the Iberian Atlantic environment).

441 Estimates of S for height were consistent across years and environments. However, S
442 estimated for tree survival was only significant in the Iberian Atlantic environment. For
443 phenology-related traits, S was significant only for bud burst measured in 2017 (Figure 5).
444 These results contrast with the consistent level of polygenicity for all these traits across years
445 and environments. Interestingly, our results suggest a stable polygenic architecture, but an
446 environment and year-dependent impact of negative selection at some traits.

447 *Gene function enrichment at pathway level*

448 Tests for gene function enrichment at the pathway level provided significant results for
449 survival in the Iberian Atlantic environment, phenology-related and biotic-stress response
450 traits, and height in the French Atlantic and Mediterranean environments. Genes coding for
451 *transcription factors* showed higher probability of being included in the VSR models
452 (*maxpostprb*) and higher estimated SNP effect-sizes (*maxabsbetarb*) for survival in the
453 Iberian Atlantic environment (Table 2). Two gene sets associated to bud burst in 2015 showed
454 signals of polygenic selection: *monolignol biosynthesis*, which had high overall values of both
455 *maxpostprb* and *maxabsbetarb*, and *glycan metabolism*, which showed low overall
456 *maxabsbetarb* estimates (Table 2). Furthermore, phenology growth index was associated with
457 enrichment for genes related to *cell growth and death*, *DNA recombination and repair* and *UV*
458 *response*, which mostly have low *maxabsbetarb* values (Table 2). *D. sapinea* susceptibility

459 was associated with enrichment of genes, with high overall *maxabsbetarb* and *maxpostprb*, in
460 the *ubiquitin system* for *D. sapinea* necrosis, and in the *signal transduction* and *flavonoid*
461 *biosynthesis* gene sets for *D. sapinea* needle discoloration (Table 2). Interestingly, height was
462 enriched for genes from different pathways when measured in contrasting environments. For
463 instance, in the French Atlantic environment genes coding for *transcription factors* showed
464 high *maxabsbetarb* and *maxpostprb*, while genes within the *cytoskeleton* pathway showed
465 overall low *maxabsbetarb* values in the Mediterranean environment.

466 **Discussion**

467 Unraveling the genetic architecture of adaptive traits is challenging because of the difficulty
468 to identify variants with small effect-sizes using GWAS. Here, we addressed this challenge
469 obtaining precise phenotypic information (over 12,500 trees were evaluated) for an extensive
470 number of fitness-related traits measured on clonal replicates. Specifically, we tested if a high
471 proportion of the genetic variance of fitness-related traits in a long-lived forest tree (maritime
472 pine) can be explained by a large number of small size-effect variants, in line with the
473 polygenic adaptation model. We also tested whether negative selection is pervasive for such
474 polygenic traits. Our results showed patterns of local adaptation for most of the analyzed
475 traits, highlighting its relationship with fitness, and also revealed a high and remarkably stable
476 degree of polygenicity, across traits, years, and environments. Moreover, using two
477 complementary multilocus approaches we accounted for a considerable proportion of the
478 heritability estimated for these highly polygenic traits, and identified negative selection as a
479 key driver of local adaptation.

480 *Evidence of local adaptation in maritime pine*

481 All phenotypic categories presented significant within-population genetic variation (i.e.
482 broad-sense heritability), and were consequently susceptible to respond to natural selection

483 (Visscher *et al.* 2008). Estimates of heritability were consistent with previous results for these
484 traits in forest trees (reviewed by Lind *et al.* 2018). In addition, our results were consistent
485 with adaptive differentiation ($Q_{ST} > F_{ST}$) for 11 out of 26 analyzed traits, involving four out of
486 the five trait categories (no evidence for survival traits). These results are in accordance with
487 reports of pervasive local adaptation in forest trees (Savolainen *et al.* 2007, 2013; Alberto *et*
488 *al.* 2013; Lind *et al.* 2018).

489 The stability of Q_{ST} estimates for height across environments and years highlights the strength
490 of directional selection for height in this species; a trait that can thus be used for the
491 delimitation of conservation and management units (Rodríguez-Quilón *et al.* 2016).
492 Contrarily, phenology-related traits showed contrasting estimates of Q_{ST} depending on the
493 environment and year of measurement. This result highlights that the evolutionary forces
494 driving population genetic differences in phenology-related traits are environmentally and
495 temporally-dependent, which can slow-down attaining phenotypic optima under rapidly
496 changing climates. Polygenic adaptation could be specially relevant for these traits because it
497 can produce rapid phenotypic changes, as it only requires small adjustments in allele
498 frequencies in the contributing loci rather than selective sweeps on new mutations (Jain and
499 Stephan 2017; Dayan *et al.* 2019; Wisser *et al.* 2019).

500 Unexpectedly, survival, a trait directly related with a component of fitness (i.e. viability), did
501 not show evidence of local adaptation in maritime pine. The low levels of phenotypic
502 variability observed for survival in this study may explain these results. Future studies should
503 focus on quantitative evaluations of survival (e.g. adding a time-frame, such as time until
504 death or order of dead trees) to better gather the complexity of this trait, and be able to discern
505 genetic differences among populations. The strong selective pressure in the Mediterranean
506 region exacerbated genetic differences in survival among clones and resulted in slightly
507 higher estimates of heritability (similarly to Gaspar *et al.* 2013). Additionally, we observed

508 significant phenotypic plasticity for height and survival, the two traits measured in all five
509 experimental sites. While our results hinted a heritable component for plasticity, this question
510 still deserves further investigation to elucidate the importance of phenotypic plasticity in the
511 adaptive response of maritime pine to changing environmental conditions (Alía *et al.* 2014;
512 Vizcaíno-Palomar *et al.* 2019).

513 Two traits in particular had remarkably high levels of adaptive genetic differentiation among
514 populations, $\delta^{13}\text{C}$ and *D. sapinea* necrosis (Figure 1), but genetic variation within populations
515 was low, compromising their adaptive potential. These traits deserve special attention because
516 of the implication of water-use efficiency in drought resistance (reviewed by Plomion *et al.*
517 2016a) and the new pathogenic outbreaks of *D. sapinea* expected on maritime pine
518 plantations fostered by climate change (Fabre *et al.* 2011; Brodde *et al.* 2019). In contrast to
519 our findings, a lack of adaptive genetic differentiation for $\delta^{13}\text{C}$ was previously reported for
520 maritime pine by Lamy *et al.* (2011), as well as for broad-leaved trees (Torres-Ruiz *et al.*
521 2019). Although this disagreement may be influenced by the much larger number of
522 populations we analyzed (see Whitlock and Guillaume 2009) as compared to Lamy *et al.*
523 (2011), we cannot rule out discrepancies due to the estimation of total genetic variance in our
524 study (i.e. based on clones), instead of additive genetic variance. Nevertheless, non-additive
525 genetic effects in maritime pine traits related to drought resistance have been reported to be of
526 little importance (Gaspar *et al.* 2013), and they should not have affected our estimates.

527 *Genetic architecture (polygenicity) of fitness-related traits*

528 Most traits assessed had a considerable degree of polygenicity, ranging between 4-15%,
529 which is on the same order of magnitude as for humans (Zeng *et al.* 2018). Polygenicity was
530 relatively similar across all analyzed traits and therefore did not depend on the level of genetic
531 control, as estimated by heritability through quantitative genetic analysis. Mei *et al.* (2018)

532 observations in humans predicted different genetic architectures as a function of genome size.
533 Surprisingly, although the maritime pine genome is more than seven times larger than that of
534 humans (De La Torre *et al.* 2014), we found similar estimates of polygenicity between both
535 species. The distributions of SNP effect-sizes showed that hundreds of SNPs with near-zero
536 effect-size contributed together to shape phenotypic differences among clones. This highly
537 polygenic architecture could be explained by the omnigenic model (Boyle *et al.* 2017).
538 Indeed, as in humans, we expect high biological complexity and interconnectivity of gene
539 expression networks in forest trees, resulting in the association of virtually all expressed genes
540 in relevant tissues with the observed phenotypes (Wray *et al.* 2018). However, this
541 explanation would not account for the lack of high effect-size SNPs in our data set composed
542 mostly of SNPs from candidate genes (see below).

543 The implementation of polygenic adaptation studies outside of humans is slowly emerging
544 (Csilléry *et al.* 2014; He *et al.* 2016; Lind *et al.* 2017; Barghi *et al.* 2019; Friedline *et al.* 2019;
545 Wisser *et al.* 2019), providing increased evidence that polygenic adaptation in complex traits
546 may be pervasive (Sella and Barton 2019). As a result, new evolutionary questions relevant
547 for different organisms are arising. For instance, in forest trees, for which local adaptation is
548 frequently observed (Savolainen *et al.* 2007, 2013; Alberto *et al.* 2013; this study), the
549 contribution of alleles with small effect-size and selection coefficients (and therefore more
550 prompted to be swamped by gene flow) to shaping local adaptation is a question that remains
551 open (Yeaman 2015). Another fundamental question, in particular for conifers, is the role of
552 genetic redundancy. It has been suggested that genetic redundancy favors polygenic
553 adaptation and speed up the achievement of phenotypic optima through multiple genetic
554 pathways leading to similar phenotypes (Höllinger *et al.* 2019; Barghi *et al.* 2019).
555 Unraveling this relationship in conifers, whose genomes are characterized by a high number
556 of paralogs (Diaz-Sala *et al.* 2013), may shed new light about how rapidly these taxa can

557 adapt to environmental changes. Moreover, the influence of genome size in the genetic
558 architecture of fitness-related traits, as well as the relationship between heritability and
559 polygenicity, deserve further investigation including a better coverage of conifer genomes, as
560 well as improved knowledge of non-coding regions (Mackay *et al.* 2012).

561 Recent studies in human height (a classic example of polygenic adaption) have suggested that
562 detecting polygenicity may be affected by subtle biases in GWAS caused by population
563 structure (Berg *et al.* 2019a; Sohail *et al.* 2019). In our study, the clonal common garden
564 network allowed separating the genetic and the environmental effect on phenotypes to
565 identify which traits are contributing to adaptation. In addition, we corrected the BLUPs
566 estimates for the effect of neutral population genetic structure. In this sense, our work
567 highlights the potential of combining precise estimation of the genetic effect on phenotypes
568 with multi-locus genotype-phenotype association models to elucidate the mechanisms that
569 allow the maintenance of genetic variation in adaptive traits, especially in species with
570 complex demographic history. Undoubtedly, next steps to decipher polygenic adaptation in
571 species with varied life-history traits should implement upcoming polygenic association
572 methods that directly correct for population stratification (e.g. Josephs *et al.* 2019).

573 *Performance of polygenic adaptation approaches (VSR and MLM)*

574 We evaluated the performance of polygenic approaches (VSR and MLM) through the
575 comparison of SNP-based genetic variance estimates, GEV. Despite some slight differences,
576 notably for biotic-stress response traits that were limited by low sample sizes, both methods
577 were robust and provided consistent estimations. The large proportion of the genetic variance
578 explained by SNP-based models, usually higher than 50%, suggests that, by adopting a
579 polygenic analytical model, we were able to account for a significant part of the heritability
580 inferred through pedigree-based analysis, even when using a modest number of SNPs. It is

581 worth noting that the performance of polygenic models did not depend on the estimated
582 degree of heritability, as evidenced by the absence of correlation between *GEV* and H^2 ($\rho =$
583 0.04 for VSR, $\rho = -0.05$ for MLM, $p > 0.05$ in both cases). For instance, polygenic models
584 allowed to explain around 45% of the broad-sense heritability, also for low-heritable traits,
585 such as survival in Mediterranean sites, polycyclism, and SLA. *GEV* can be interpreted as an
586 analogous of the SNP-based heritability, with the particularity that *GEV* refers to proportion
587 of the variance in genetic values, rather than on the phenotypic values that are explained by
588 associated SNPs (see Materials and Methods for further details). SNP-based heritability is
589 becoming a fundamental parameter in quantitative genetics because it can yield insights into
590 the ‘missing heritability’ of complex traits (Hou *et al.* 2019). In this sense, our study shows
591 that polygenic approaches can be a promising strategy to account for a significant part of this
592 missing heritability that is commonly observed in GWAS in forest trees (reviewed by Hall *et*
593 *al.* 2016; Lind *et al.* 2018).

594 However, insights provided by SNP-based estimations of *GEV* should be interpreted with
595 caution. First, because maritime pine has a huge genome size (around 28 Gbp; Grotkopp *et al.*
596 2004; Zonneveld 2012) and a rapid decay in linkage disequilibrium (Neale and Savolainen
597 2004), a larger number of genotyped SNPs should be needed to obtain a good genomic
598 coverage. And second, because rare variants are usually difficult to incorporate in genotyping
599 platforms, such as the one used in our study. Such rare variants may indeed account for an
600 important proportion of the heritability in complex traits (Young 2019). Even though further
601 investigations are needed to draw stronger conclusions, robust and consistent estimates of
602 polygenicity across methods were fostered herein by a precise phenotypic evaluation in a
603 large number of individuals (over 12,500 trees).

604 *Stability of polygenicity estimates across environments and years*

605 The temporal and spatial heterogeneity of selection can impact the evolution of the genetic
606 architecture underlying adaptation (Sella and Barton 2019). Monitoring the patterns of genetic
607 architecture not only across environments but also across years is an important issue in long-
608 lived forest trees that may experience changing selection pressures along their lifetimes. In
609 this sense, our study is not only a validation of the polygenic adaptation model in a new
610 organism, but a contribution to improving our understanding of adaptation. Surprisingly, the
611 estimated degree of polygenicity remained stable across environments for all trait categories,
612 especially tree height. Additionally, we observed highly stable genetic architectures for
613 height, phenology, and survival across years. For the case of tree height, polygenicity was
614 highly stable for three time-point measures along a time-span of 6 years, comprising seedling
615 and juvenile stages, during which trees are more vulnerable and selection pressure are more
616 pronounced (Leck *et al.* 2008). However, analysis of gene function enrichment (see below)
617 suggests that different genetic pathways could be underlying phenotypic variation in
618 contrasting environments. Moreover, differences in gene expression may also underlie
619 adaptation under different environments and years (Mähler *et al.* 2017; Hämälä *et al.* 2020) .

620 *The role of negative selection in polygenic adaptation*

621 All significant correlations between SNP effect-size and MAF were negative (for tree height,
622 bud burst and SLA), suggesting a genetic architecture modeled, at least partially, by the action
623 of negative selection, i.e. SNPs with large effects are rare because they mostly have
624 deleterious effects and are thus selected against (O'Connor *et al.* 2019). The MLM method
625 did not allow elucidating whether negative estimates of S were the consequence of an
626 enrichment of trait-increasing or trait-decreasing alleles (Zeng *et al.* 2018), but it certainly
627 suggests that these traits have been under some form of negative selection. The effect of
628 purifying selection is widespread in model plant genomes (Wright and Andolfatto 2008), and
629 it has been largely evidenced in trees (Krutovsky and Neale 2005; Palmé *et al.* 2009; Eckert *et*

630 *al.* 2013; De La Torre *et al.* 2017; Grivet *et al.* 2017). Indeed, negative selection, and its
631 variation across populations and through time, has been pointed out as a main cause for
632 maintaining polygenicity (Zeng *et al.* 2018; O'Connor *et al.* 2019). Thus, negative selection
633 may also explain, at least partially, the degree of polygenicity observed for fitness-related
634 traits in maritime pine (but see below), as well as the absence of large effect-size SNPs in
635 previous association studies for this species (Lepoittevin *et al.* 2012; Budde *et al.* 2014; Hurel
636 *et al.* 2019).

637 Nevertheless, strikingly, the negative selection patterns observed across environments and
638 years did not mimic the trend observed for polygenicity. That is, negative selection was
639 consistently inferred for height, but its strength changed across environments and years for
640 survival and phenology-related traits. This uncoupling between negative selection and
641 polygenicity may result from the fact that our limited coverage of maritime pine genome did
642 not account for (most) rare variants, which can considerably affect S estimates (Zeng *et al.*
643 2018). In addition, polygenic adaptation generally results in highly stochastic genetic
644 responses driven by non-predictable changes in allele frequencies (Zhang *et al.* 2013).

645 Finally, we detected signals of gene enrichment for 10 pathways that had higher values of
646 maximum SNP effect-size or higher posterior probability of being included in the polygenic
647 models: height in the French Atlantic environment and survival in the Iberian Atlantic
648 environment were enriched for genes coding for *transcription factors*, bud burst in 2015 for
649 genes within the *monolignol biosynthesis* pathway, and *D. sapinea* susceptibility (considering
650 both the induced necrosis and needle discoloration) for genes within the *ubiquitin system*,
651 *signal transduction* and *flavonoid biosynthesis* pathways. Assuming that evolution of these
652 pathways is driven by negative selection, these patterns could be interpreted as a consequence
653 of the accumulation of (slightly) deleterious alleles, resulting in higher proportions of SNPs
654 with non-zero effect-size on these phenotypic traits. This higher tolerance to retain deleterious

655 mutations could be explained by a high genetic redundancy (Nowak *et al.* 1997; Krakauer and
656 Nowak 1999). Otherwise, if we were to assume a higher impact of positive than negative
657 selection, the observed patterns would imply an accumulation of beneficial mutations in these
658 pathways, which is a hypothesis worth exploring using sequence-based neutrality tests in
659 future studies.

660 Another five pathways were enriched in lower effect-sizes alleles: genes involved in
661 *cytoskeleton* were linked with height in the Mediterranean environment, those in the *glycan*
662 *metabolism* pathway were associated with bud burst in 2015, and those for *cell growth and*
663 *death, DNA recombination and repair, and UV response* were associated with phenology
664 growth index. These pathways perform general functions and could be constituted by
665 functionally important genes. In this case, the observed patterns suggest higher genetic
666 constraints on these functionally important genes, for which negative selection should be
667 highly efficient (Wright and Andolfatto 2008). Interestingly, our results suggest that even for
668 stable estimates of polygenicity, different gene pathways could underlie polygenic adaptation
669 for height in contrasting environments. Finally, although our gene enrichment analysis
670 revealed some pathways with stronger evidence for polygenic adaptation, we cannot discard
671 the influence of other (non-studied) gene pathways, as pointed by the omnigenic theory
672 (Boyle *et al.* 2017).

673 **Conclusions**

674 The study of genetic adaptation is currently facing new challenges. The advancement of
675 GWAS relies on the development of methods able to detect causal variants of small effect-
676 size, or at low allele frequencies. Our study, adopting a polygenic adaptation model on well-
677 characterized maritime pine clones planted in contrasted environments, contributed to a better
678 understanding of the heritability of complex adaptive traits in long-lived organisms, and its

679 underlying genetic architecture. Our results showed that most complex adaptive traits are
680 polygenic, with several of them showing also signatures of negative selection. The degree of
681 polygenicity was similar for traits spanning different functional categories, and this genetic
682 architecture was considerably stable over time and across environments. Current models for
683 predicting population trajectories in forest trees under climate change are based on
684 identification of outlier SNPs with relatively large effects on phenotypes and/or strong
685 correlation with climate variables (e.g. Jaramillo-Correa *et al.* 2015; Rellstab *et al.* 2016; Lu
686 *et al.* 2019). Because polygenic adaptation can take place rapidly (see, for example, Jain and
687 Stephan 2017), current prediction models are probably underestimating the capacity of natural
688 forest tree populations to adapt to new environments. Thus, adopting a polygenic adaptation
689 perspective could significantly improve prediction accuracy, and provide new scenarios to
690 inform forest conservation and reforestation programs (Valladares *et al.* 2014; Fady *et al.*
691 2016). Also, a better understanding of the genetic architecture of economically valuable
692 polygenic traits can improve genomic-assisted breeding, and allow building better genomic
693 selection models (Grattapaglia *et al.* 2018).

694 **Acknowledgements**

695 We thank A. Saldaña, F. del Caño, E. Ballesteros and D. Barba (INIA) and the ‘Unité
696 Expérimentale Forêt Pierrot’ (UEFP, INRAE; doi: 10.15454/1.5483264699193726E12) for
697 field assistance. Data used in this research are part of the Spanish Network of Genetic Trials
698 (GENFORED, <http://www.genfored.es>). We thank all persons and institutions linked to the
699 establishment and maintenance of field trials used in this study. Thanks are extended to
700 Antoine Kremer, Martin Lascoux and Outi Savolainen for valuable insights and discussions
701 on models of local adaptation in forest trees.

702 **Funding**

703 This study was funded by the Spanish Ministry of Economy and Competitiveness through
704 projects RTA2010-00120-C02-02 (CLONAPIN), CGL2011-30182-C02-01 (AdapCon) and
705 AGL2012-40151-C03-02 (FENOPIN). The study was also supported by the ‘Initiative
706 d’Excellence (IdEx) de l’Université de Bordeaux - Chaires d’installation 2015’ (EcoGenPin)
707 and the European Union’s Horizon 2020 research and innovation programme under grant
708 agreement No 773383 (B4EST).

709 **Author contributions**

710 Mde-M collected field data, carried out the statistical analyses and drafted the manuscript.
711 JM, RA and CP designed and established the common gardens, and helped with field data
712 collection. IR-Q, DG, CP, GGV and SCG-M contributed to the SNP assay design and
713 molecular laboratory work. AE, RA and SCG-M conceived and designed the study. IR-Q and
714 AH collected field data and helped with the statistical analyses. JPJ-C identified gene
715 pathways and defined gene-sets. MH, SCG-M, DG, JPJ-C and GGV contributed to the
716 statistical analysis of genomic data. SCG-M coordinated the study. All authors contributed to
717 manuscript discussion and review, and gave final approval for publication.

718 **Supplemental material**

719 **Table S1. Phenotypic data summary and quantitative genetic analysis.** V_g stands for
720 genetic variance (posterior mean of the variance explained by clone effect), H^2 stands for
721 broad-sense heritability and Q_{ST} for genetic differentiation among populations (posterior mode
722 and 95% credible interval are presented).

723 **Table S2. MCMCglmm Bayesian model parametrization.** Psrf stands for the Gelman-
724 Rubin potential scale reduction factor criterion, a measure of model convergence. Good
725 convergence of models is expected for $psrf < 1.02$.

726 **Table S3. List of genes included in the 17 gene sets considered for gene function**
727 **enrichment at pathway level.** Annotation based on KEGG: Kyoto Encyclopedia of Genes
728 and Genomes (<https://www.genome.jp/kegg/>) is also provided. *Annotation* label indicates
729 genes for which no hit with KEGG database was found and thus were assigned to metabolic
730 pathways/modules based on the InterPro annotation.

731 **Table S4. Number of non-zero effect-size SNPs (*nbnon-zero*) and genetic explained**
732 **variance (GEV) estimated using Bayesian variable selection regression (VSR), as**
733 **implemented in piMASS software, and the Bayesian linear mixed model, MLM,**
734 **implemented in GCTB software.** For MLM, the coefficients of correlation between SNP
735 effect-size and minor allele frequency (S) are also provided. The parameters are presented as
736 the posterior median and 95% credible intervals. Estimates not overlapping zero are marked
737 in bold. NA: models that did not converge.

738 **Figure S1. Sampled maritime pine populations (circles) and common garden sites (other**
739 **symbols).** Neutral gene pools (identified in Jaramillo-Correa *et al.* 2015) outline the species
740 natural distribution range in different colors.

741 **Figure S2. Posterior distribution of the number of non-zero size-effect SNPs for 26 traits**
742 **belonging to five categories: survival, height, phenology-related, functional, and biotic-**
743 **stress response traits.** The number of non-zero size-effect SNPs was estimated through two
744 Bayesian methods: posterior inference via model averaging and subset selection (VSR), as
745 implemented in the software piMASS (Guan and Stephens 2011), and the Mixed Linear
746 Model (MLM) implemented in the software CGTB (Zeng *et al.* 2018). The posterior median
747 is indicated with a dashed line.

748 **Figure S3. Posterior distribution of SNP effect-sizes for 26 traits belonging to five**
749 **categories: survival, height, phenology-related, functional, and biotic-stress response**

750 **traits.** SNP effect-size was estimated through two Bayesian methods: posterior inference via
751 model averaging and subset selection (VSR), as implemented in the software piMASS (Guan
752 and Stephens 2011), and the Mixed Linear Model (MLM) implemented in the software CGTB
753 (Zeng *et al.* 2018).

754

755 Literature cited

756 Alberto F. J., S. N. Aitken, R. Alía, S. C. González-Martínez, H. Hänninen, *et al.*, 2013
757 Potential for evolutionary responses to climate change – evidence from tree populations. *Glob*
758 *Chang Biol* 19: 1645–1661. <https://doi.org/10.1111/gcb.12181>

759 Alía R., R. Chambel, E. Notivol, J. Climent, and S. C. González-Martínez, 2014
760 Environment-dependent microevolution in a Mediterranean pine (*Pinus pinaster* Aiton). *BMC*
761 *Evol Biol* 14: 200. <https://doi.org/10.1186/s12862-014-0200-5>

762 Alonso-Blanco C., J. Andrade, C. Becker, F. Bemm, J. Bergelson, *et al.*, 2016 1,135 Genomes
763 Reveal the Global Pattern of Polymorphism in *Arabidopsis thaliana*. *Cell* 166: 481–491.
764 <https://doi.org/10.1016/j.cell.2016.05.063>

765 Aranda I., R. Alía, U. Ortega, Á. K. Dantas, and J. Majada, 2010 Intra-specific variability in
766 biomass partitioning and carbon isotopic discrimination under moderate drought stress in
767 seedlings from four *Pinus pinaster* populations. *Tree Genet Genomes* 6: 169–178.
768 <https://doi.org/10.1007/s11295-009-0238-5>

769 Barghi N., R. Tobler, V. Nolte, A. M. Jakšić, F. Mallard, *et al.*, 2019 Genetic redundancy
770 fuels polygenic adaptation in *Drosophila*. *PLoS Biol.* 17: e3000128.
771 <https://doi.org/10.1371/journal.pbio.3000128>

772 Berg J. J., and G. Coop, 2014 A Population Genetic Signal of Polygenic Adaptation. *PLoS*
773 *Genetics* 10: e1004412. <https://doi.org/10.1371/journal.pgen.1004412>

774 Berg J. J., A. Harpak, N. Sinnott-Armstrong, A. M. Joergensen, H. Mostafavi, *et al.*, 2019a
775 Reduced signal for polygenic adaptation of height in UK Biobank. *eLife* 8: e39725.
776 <https://doi.org/10.7554/eLife.39725>

777 Berg J. J., X. Zhang, and G. Coop, 2019b Polygenic Adaptation has Impacted Multiple
778 Anthropometric Traits. *bioRxiv* 167551. <https://doi.org/10.1101/167551>

779 Bernatchez S., A. Xuereb, M. Laporte, L. Benestan, R. Steeves, *et al.*, 2019 Seascape
780 genomics of eastern oyster (*Crassostrea virginica*) along the Atlantic coast of Canada. *Evol.*
781 *Appl.* 12: 587–609. <https://doi.org/10.1111/eva.12741>

782 Björkegren J. L. M., J. C. Kovacic, J. T. Dudley, and E. E. Schadt, 2015 Genome-Wide
783 Significant Loci: How Important Are They? *J Am Coll Cardiol* 65: 830–845.
784 <https://doi.org/10.1016/j.jacc.2014.12.033>

785 Boyle E. A., Y. I. Li, and J. K. Pritchard, 2017 An Expanded View of Complex Traits: From
786 Polygenic to Omnipotent. *Cell* 169: 1177–1186. <https://doi.org/10.1016/j.cell.2017.05.038>

787 Brachi B., G. P. Morris, and J. O. Borevitz, 2011 Genome-wide association studies in plants:
788 the missing heritability is in the field. *Genome Biol.* 12: 232. <https://doi.org/10.1186/gb-2011-12-10-232>

790 Brendel O., 2001 Does bulk-needle $\delta^{13}\text{C}$ reflect short-term discrimination? *Ann. For. Sci.* 58:
791 135–141.

792 Brodde L., K. Adamson, J. Julio Camarero, C. Castaño, R. Drenkhan, *et al.*, 2019 *Diplodia*

793 Tip Blight on Its Way to the North: Drivers of Disease Emergence in Northern Europe. *Front*
794 *Plant Sci* 9: 1818. <https://doi.org/10.3389/fpls.2018.01818>

795 Bucci G., S. C. González-Martínez, G. L. Provost, C. Plomion, M. M. Ribeiro, *et al.*, 2007
796 Range-wide phylogeography and gene zones in *Pinus pinaster* Ait. revealed by chloroplast
797 microsatellite markers. *Mol Ecol* 16: 2137–2153. <https://doi.org/10.1111/j.1365-294X.2007.03275.x>

799 Budde K. B., M. Heuertz, A. Hernández-Serrano, J. G. Pausas, G. G. Vendramin, *et al.*, 2014
800 In situ genetic association for serotiny, a fire-related trait, in Mediterranean maritime pine
801 (*Pinus pinaster*). *New Phytol* 201: 230–241. <https://doi.org/10.1111/nph.12483>

802 Canales J., R. Bautista, P. Label, J. Gómez-Maldonado, I. Lesur, *et al.*, 2014 De novo
803 assembly of maritime pine transcriptome: implications for forest breeding and biotechnology.
804 *Plant Biotechnol. J.* 12: 286–99. <https://doi.org/10.1111/pbi.12136>

805 Craine J. M., E. N. J. Brookshire, M. D. Cramer, N. J. Hasselquist, K. Koba, *et al.*, 2015
806 Ecological interpretations of nitrogen isotope ratios of terrestrial plants and soils. *Plant Soil*
807 396: 1–26. <https://doi.org/10.1007/s11104-015-2542-1>

808 Csilléry K., H. Lalagüe, G. G. Vendramin, S. C. González-Martínez, B. Fady, *et al.*, 2014
809 Detecting short spatial scale local adaptation and epistatic selection in climate-related
810 candidate genes in European beech (*Fagus sylvatica*) populations. *Mol Ecol* 23: 4696–4708.
811 <https://doi.org/10.1111/mec.12902>

812 Daub J. T., T. Hofer, E. Cutivet, I. Dupanloup, L. Quintana-Murci, *et al.*, 2013 Evidence for
813 Polygenic Adaptation to Pathogens in the Human Genome. *Mol Biol Evol* 30: 1544–1558.
814 <https://doi.org/10.1093/molbev/mst080>

815 Dayan D. I., X. Du, T. Z. Baris, D. N. Wagner, D. L. Crawford, *et al.*, 2019 Population
816 genomics of rapid evolution in natural populations: polygenic selection in response to power
817 station thermal effluents. *BMC Evol. Biol.* 19: 61. <https://doi.org/10.1186/s12862-019-1392-5>

818 De La Torre A. R., I. Birol, J. Bousquet, P. K. Ingvarsson, S. Jansson, *et al.*, 2014 Insights
819 into conifer giga-genomes. *Plant Physiol.* 166: 1724–32.
820 <https://doi.org/10.1104/pp.114.248708>

821 De La Torre A. R., Z. Li, Y. Van de Peer, and P. K. Ingvarsson, 2017 Contrasting Rates of
822 Molecular Evolution and Patterns of Selection among Gymnosperms and Flowering Plants.
823 *Mol. Biol. Evol.* 34: 1363–1377. <https://doi.org/10.1093/molbev/msx069>

824 De La Torre A. R., B. Wilhite, and D. B. Neale, 2019 Environmental Genome-Wide
825 Association Reveals Climate Adaptation Is Shaped by Subtle to Moderate Allele Frequency
826 Shifts in Loblolly Pine. *Genome Biol Evol* 11: 2976–2989.
827 <https://doi.org/10.1093/gbe/evz220>

828 Desprez-Loustau M.-L., B. Marçais, L.-M. Nageleisen, D. Piou, and A. Vannini, 2006
829 Interactive effects of drought and pathogens in forest trees. *Ann. For. Sci.* 63: 597–612.
830 <https://doi.org/10.1051/forest:2006040>

831 Díaz S., J. Kattge, J. H. C. Cornelissen, I. J. Wright, S. Lavorel, *et al.*, 2016 The global
832 spectrum of plant form and function. *Nature* 529: 167–171.

833 <https://doi.org/10.1038/nature16489>

834 Diaz-Sala C., J. A. Cabezas, B. Fernández de Simón, D. Abarca, M. Á. Guevara, *et al.*, 2013
835 The uniqueness of conifers, pp. 67–96 in *From Plant Genomics to Plant Biotechnology*,
836 edited by Poltronieri P., Burbulis N., Fogher C. Woodhead Publishing, Cambridge.

837 Eckert A. J., A. D. Bower, K. D. Jermstad, J. L. Wegrzyn, B. J. Knaus, *et al.*, 2013 Multilocus
838 analyses reveal little evidence for lineage-wide adaptive evolution within major clades of soft
839 pines (*Pinus* subgenus *Strobus*). *Mol Ecol* 22: 5635–5650. <https://doi.org/10.1111/mec.12514>

840 Edge M. D., and G. Coop, 2019 Reconstructing the History of Polygenic Scores Using
841 Coalescent Trees. *Genetics* 211: 235–262. <https://doi.org/10.1534/genetics.118.301687>

842 Fabre B., D. Piou, M.-L. Desprez-Loustau, and B. Marçais, 2011 Can the emergence of pine
843 Diplodia shoot blight in France be explained by changes in pathogen pressure linked to
844 climate change? *Glob Chang Biol* 17: 3218–3227. <https://doi.org/10.1111/j.1365-2486.2011.02428.x>

845 Fady B., J. Cottrell, L. Ackzell, R. Alía, B. Muys, *et al.*, 2016 Forests and global change:
846 what can genetics contribute to the major forest management and policy challenges of the
847 twenty-first century? *Reg Environ Change* 16: 927–939. <https://doi.org/10.1007/s10113-015-0843-9>

848 Farquhar G. D., and R. A. Richards, 1984 Isotopic Composition of Plant Carbon Correlates
849 With Water-Use Efficiency of Wheat Genotypes. *Functional Plant Biol.* 11: 539–552.
<https://doi.org/10.1071/PP9840539>

850 Field Y., E. Boyle, N. Telis, Z. Gao, K. J. Gaulton, *et al.*, 2016 Detection of human adaptation
851 during the past 2000 years. *Science* 354: 760–764. <https://doi.org/10.1126/science.aah5114>

852 Fisher R. A., 1918 The correlation between relatives on the supposition of Mendelian
853 inheritance. *Transaction Royal Society Edinburgh* 52: 399–433.

854 Fréjaville T., and M. Benito Garzón, 2018 The EuMedClim Database: Yearly Climate Data
855 (1901–2014) of 1 km Resolution Grids for Europe and the Mediterranean Basin. *Front. Ecol.*
856 *Evol.* 6: 31. <https://doi.org/10.3389/fevo.2018.00031>

857 Friedline C. J., T. M. Faske, B. M. Lind, E. M. Hobson, D. Parry, *et al.*, 2019 Evolutionary
858 genomics of gypsy moth populations sampled along a latitudinal gradient. *Mol. Ecol.* 28:
859 2206–2223. <https://doi.org/10.1111/mec.15069>

860 Gaspar M. J., T. Velasco, I. Feito, R. Alía, and J. Majada, 2013 Genetic Variation of Drought
861 Tolerance in *Pinus pinaster* at Three Hierarchical Levels: A Comparison of Induced Osmotic
862 Stress and Field Testing. *PLOS ONE* 8: e79094.
<https://doi.org/10.1371/journal.pone.0079094>

863 Gelman A., and D. B. Rubin, 1992 Inference from iterative simulation using multiple
864 sequences. *Stat Sci* 7: 457–511.

865 Gelman A., 2006 Prior distributions for variance parameters in hierarchical models (comment
866 on article by Browne and Draper). *Bayesian Anal* 1: 515–534. <https://doi.org/10.1214/06-BA117A>

872 Gelman A., D. A. van Dyk, Z. Huang, and Boscardin, 2008 Using Redundant
873 Parameterizations to Fit Hierarchical Models. *J Comput Graph Stat* 17: 95–122.

874 Girard F., M. Vennetier, S. Ouarmim, Y. Caraglio, and L. Misson, 2011 Polycyclism, a
875 fundamental tree growth process, decline with recent climate change: the example of *Pinus*
876 *halepensis* Mill. in Mediterranean France. *Trees* 25: 311–322. <https://doi.org/10.1007/s00468-010-0507-9>

878 Gneccchi-Ruscone G. A., P. Abondio, S. De Fanti, S. Sarno, M. G. Sherpa, *et al.*, 2018
879 Evidence of Polygenic Adaptation to High Altitude from Tibetan and Sherpa Genomes.
880 *Genome Biol Evol* 10: 2919–2930. <https://doi.org/10.1093/gbe/evy233>

881 González-Martínez S. C., R. Alía, and L. Gil, 2002 Population genetic structure in a
882 Mediterranean pine (*Pinus pinaster* Ait.): a comparison of allozyme markers and quantitative
883 traits. *Heredity* 89: 199–206. <https://doi.org/10.1038/sj.hdy.6800114>

884 González-Martínez S. C., K. V. Krutovsky, and D. B. Neale, 2006 Forest-tree population
885 genomics and adaptive evolution. *New Phytol* 170: 227–238.

886 Grattapaglia D., O. B. Silva-Junior, R. T. Resende, E. P. Cappa, B. S. F. Müller, *et al.*, 2018
887 Quantitative Genetics and Genomics Converge to Accelerate Forest Tree Breeding. *Front.*
888 *Plant Sci.* 9: 1693. <https://doi.org/10.3389/fpls.2018.01693>

889 Greenwood S., P. Ruiz-Benito, J. Martínez-Vilalta, F. Lloret, T. Kitzberger, *et al.*, 2017
890 Tree mortality across biomes is promoted by drought intensity, lower wood density and
891 higher specific leaf area. *Ecol Lett* 20: 539–553. <https://doi.org/10.1111/ele.12748>

892 Grivet D., K. Avia, A. Vaattovaara, A. J. Eckert, D. B. Neale, *et al.*, 2017 High rate of
893 adaptive evolution in two widespread European pines. *Mol Ecol* 26: 6857–6870.
894 <https://doi.org/10.1111/mec.14402>

895 Grotkopp E., M. Rejmánek, M. J. Sanderson, and T. L. Rost, 2004 Evolution of Genome Size
896 in Pines (*Pinus*) and Its Life-History Correlates: Supertree Analyses. *Evolution* 58: 1705.
897 <https://doi.org/10.1554/03-545>

898 Guan Y., and M. Stephens, 2011 Bayesian variable selection regression for genome-wide
899 association studies and other large-scale problems. *Ann Appl Stat* 5: 1780–1815.
900 <https://doi.org/10.1214/11-AOAS455>

901 Hadfield J. D., 2010 MCMC Methods for Multi-Response Generalized Linear Mixed Models:
902 The **MCMCglmm** *R* Package. *Journal of Statistical Software* 33.
903 <https://doi.org/10.18637/jss.v033.i02>

904 Hall T., 1999 BioEdit: a user-friendly biological sequence alignment editor and analysis
905 program for Window 95/98/NT. *Nucleic Acids Symposium Series* 41: 95–98.

906 Hall D., H. R. Hallingbäck, and H. X. Wu, 2016 Estimation of number and size of QTL
907 effects in forest tree traits. *Tree Genet Genomes* 12: 110. <https://doi.org/10.1007/s11295-016-1073-0>

909 Hämälä T., M. J. Guiltinan, J. H. Marden, S. N. Maximova, C. W. dePamphilis, *et al.*, 2020
910 Gene Expression Modularity Reveals Footprints of Polygenic Adaptation in *Theobroma*
911 *cacao*. *Mol Biol Evol* 37: 110–123. <https://doi.org/10.1093/molbev/msz206>

912 Hancock A. M., D. B. Witonsky, E. Ehler, G. Alkorta-Aranburu, C. Beall, *et al.*, 2010a
913 Human adaptations to diet, subsistence, and ecoregion are due to subtle shifts in allele
914 frequency. PNAS 107: 8924–8930. <https://doi.org/10.1073/pnas.0914625107>

915 Hancock A. M., G. Alkorta-Aranburu, D. B. Witonsky, and A. Di Rienzo, 2010b Adaptations
916 to new environments in humans: the role of subtle allele frequency shifts. Phil. Trans. R. Soc.
917 B 365: 2459–2468. <https://doi.org/10.1098/rstb.2010.0032>

918 Hayward L. K., and G. Sella, 2019 Polygenic adaptation after a sudden change in
919 environment. bioRxiv. <https://doi.org/10.1101/792952>

920 He F., A. L. Arce, G. Schmitz, M. Koornneef, P. Novikova, *et al.*, 2016 The Footprint of
921 Polygenic Adaptation on Stress-Responsive Cis-Regulatory Divergence in the *Arabidopsis*
922 Genus. Mol Biol Evol 33: 2088–2101. <https://doi.org/10.1093/molbev/msw096>

923 Heinzelmann R., C. Dutech, T. Tsykun, F. Labb  , J.-P. Soularue, *et al.*, 2019 Latest advances
924 and future perspectives in *Armillaria* research. Can. J. For. Res. 41: 1–23.
925 <https://doi.org/10.1080/07060661.2018.1558284>

926 Henderson C. R., 1973 Sire evaluation and genetic trends. J Anim Sci 1973: 10–41.
927 <https://doi.org/10.1093/ansci/1973.Symposium.10>

928 Hermisson J., and P. S. Pennings, 2017 Soft sweeps and beyond: understanding the patterns
929 and probabilities of selection footprints under rapid adaptation. Methods. Ecol. Evol 8: 700–
930 716. <https://doi.org/10.1111/2041-210X.12808>

931 H  llinger I., P. S. Pennings, and J. Hermisson, 2019 Polygenic adaptation: From sweeps to
932 subtle frequency shifts. PLOS Genetics 15: e1008035.

933 Hou K., K. S. Burch, A. Majumdar, H. Shi, N. Mancuso, *et al.*, 2019 Accurate estimation of
934 SNP-heritability from biobank-scale data irrespective of genetic architecture. Nat Genet 51:
935 1244–1251. <https://doi.org/10.1038/s41588-019-0465-0>

936 Huang X., and B. Han, 2014 Natural Variations and Genome-Wide Association Studies in
937 Crop Plants. Annu. Rev. Plant Biol 65: 531–551. <https://doi.org/10.1146/annurev-arplant-050213-035715>

939 Hurel A., M. de Miguel, C. Dutech, M.-L. Desprez-Loustau, C. Plomion, *et al.*, 2019 Genetic
940 basis of susceptibility to *Diplodia sapinea* and *Armillaria ostoyae* in maritime pine. bioRxiv
941 699389. <https://doi.org/10.1101/699389>

942 Jacquet J.-S., A. Bosc, A. P. O’Grady, and H. Jactel, 2013 Pine growth response to
943 processionary moth defoliation across a 40-year chronosequence. Forest Ecol Manag 293: 29–
944 38. <https://doi.org/10.1016/j.foreco.2012.12.003>

945 Jain K., and W. Stephan, 2017 Rapid Adaptation of a Polygenic Trait After a Sudden
946 Environmental Shift. Genetics 206: 389–406. <https://doi.org/10.1534/genetics.116.196972>

947 Jaramillo-Correa J.-P., I. Rodr  guez-Quil  n, D. Grivet, C. Lepoittevin, F. Sebastiani, *et al.*,
948 2015 Molecular Proxies for Climate Maladaptation in a Long-Lived Tree (*Pinus pinaster*
949 Aiton, Pinaceae). Genetics 199: 793–807. <https://doi.org/10.1534/genetics.114.173252>

950 Josephs E. B., J. J. Berg, J. Ross-Ibarra, and G. Coop, 2019 Detecting adaptive differentiation

951 in structured populations with genomic data and common gardens. *Genetics* 211: 989–1004.
952 <https://doi.org/10.1101/368506>

953 Kanehisa M., Y. Sato, and K. Morishima, 2016 BlastKOALA and GhostKOALA: KEGG
954 Tools for Functional Characterization of Genome and Metagenome Sequences. *J. Mol. Biol.*
955 428: 726–731. <https://doi.org/10.1016/j.jmb.2015.11.006>

956 Keenan K., P. McGinnity, T. F. Cross, W. W. Crozier, and P. A. Prodöhl, 2013 diveRsity: An
957 R package for the estimation and exploration of population genetics parameters and their
958 associated errors. *Methods. Ecol. Evol* 4: 782–788. <https://doi.org/10.1111/2041-210X.12067>

959 Krakauer D. C., and M. A. Nowak, 1999 Evolutionary preservation of redundant duplicated
960 genes. *Semin. Cell Dev. Biol.* 10: 555–559. <https://doi.org/10.1006/scdb.1999.0337>

961 Krutovsky K. V., and D. B. Neale, 2005 Nucleotide Diversity and Linkage Disequilibrium in
962 Cold-Hardiness- and Wood Quality-Related Candidate Genes in Douglas Fir. *Genetics* 171:
963 2029–2041. <https://doi.org/10.1534/genetics.105.044420>

964 Lamy J.-B., L. Bouffier, R. Burlett, C. Plomion, H. Cochard, *et al.*, 2011 Uniform Selection
965 as a Primary Force Reducing Population Genetic Differentiation of Cavitation Resistance
966 across a Species Range. *PLoS ONE* 6: e23476. <https://doi.org/10.1371/journal.pone.0023476>

967 Le Corre V., and A. Kremer, 2003 Genetic Variability at Neutral Markers, Quantitative Trait
968 Loci and Trait in a Subdivided Population Under Selection. *Genetics* 164: 1205–1219.

969 Leck M. A., V. T. Parker, and R. L. Simpson, 2008 *Seedling Ecology and Evolution*.
970 Cambridge University Press.

971 Lepoittevin C., L. Harvengt, C. Plomion, and P. Garnier-Géré, 2012 Association mapping for
972 growth, straightness and wood chemistry traits in the *Pinus pinaster* Aquitaine breeding
973 population. *Tree Genet Genomes* 8: 113–126. <https://doi.org/10.1007/s11295-011-0426-y>

974 Lind B. M., C. J. Friedline, J. L. Wegrzyn, P. E. Maloney, D. R. Vogler, *et al.*, 2017 Water
975 availability drives signatures of local adaptation in whitebark pine (*Pinus albicaulis* Engelm.)
976 across fine spatial scales of the Lake Tahoe Basin, USA. *Mol Ecol* 26: 3168–3185.
977 <https://doi.org/10.1111/mec.14106>

978 Lind B. M., M. Menon, C. E. Bolte, T. M. Faske, and A. J. Eckert, 2018 The genomics of
979 local adaptation in trees: are we out of the woods yet? *Tree Genet Genomes* 14: 29.
980 <https://doi.org/10.1007/s11295-017-1224-y>

981 Liu X., P.-R. Loh, L. J. O'Connor, S. Gazal, A. Schoech, *et al.*, 2018 Quantification of
982 genetic components of population differentiation in UK Biobank traits reveals signals of
983 polygenic selection. *bioRxiv* 357483. <https://doi.org/10.1101/357483>

984 Lloyd-Jones L. R., J. Zeng, J. Sidorenko, L. Yengo, G. Moser, *et al.*, 2019 Improved
985 polygenic prediction by Bayesian multiple regression on summary statistics. *Nat Commun* 10:
986 1–11. <https://doi.org/10.1038/s41467-019-12653-0>

987 Lu M., K. V. Krutovsky, and C. A. Loopstra, 2019 Predicting adaptive genetic variation of
988 loblolly pine (*Pinus taeda* L.) populations under projected future climates based on
989 multivariate models. *J Hered* 110: 857–865. <https://doi.org/10.1093/jhered/esz065>

990 Mackay J., J. F. D. Dean, C. Plomion, D. G. Peterson, F. M. Cánovas, *et al.*, 2012 Towards
991 decoding the conifer giga-genome. *Plant Mol Biol* 80: 555–69.
992 <https://doi.org/10.1007/s11103-012-9961-7>

993 Maher B., 2008 Personal genomes: The case of the missing heritability. *Nature* 456: 18–21.
994 <https://doi.org/doi:10.1038/456018a>

995 Mähler N., J. Wang, B. K. Terebieniec, P. K. Ingvarsson, N. R. Street, *et al.*, 2017 Gene co-
996 expression network connectivity is an important determinant of selective constraint. *PLOS*
997 *Genet* 13: e1006402. <https://doi.org/10.1371/journal.pgen.1006402>

998 Majada J., C. Martínez-Alonso, I. Feito, A. Kidelman, I. Aranda, *et al.*, 2011 Mini-cuttings:
999 an effective technique for the propagation of *Pinus pinaster* Ait. *New Forests* 41: 399–412.
1000 <https://doi.org/10.1007/s11056-010-9232-x>

1001 Manolio T. A., F. S. Collins, N. J. Cox, D. B. Goldstein, L. A. Hindorff, *et al.*, 2009 Finding
1002 the missing heritability of complex diseases. *Nature* 461: 747–753.
1003 <https://doi.org/10.1038/nature08494>

1004 Mayol M., M. Riba, S. Cavers, D. Grivet, L. Vincenot, *et al.*, 2020 A multiscale approach to
1005 detect selection in nonmodel tree species: Widespread adaptation despite population decline
1006 in *Taxus baccata* L. *Evol. Appl.* 0. <https://doi.org/10.1111/eva.12838>

1007 McKay J. K., and R. G. Latta, 2002 Adaptive population divergence: markers, QTL and traits.
1008 *Trends Ecol. Evol* 17: 285–291. [https://doi.org/10.1016/S0169-5347\(02\)02478-3](https://doi.org/10.1016/S0169-5347(02)02478-3)

1009 Mei W., M. G. Stetter, D. J. Gates, M. C. Stitzer, and J. Ross-Ibarra, 2018 Adaptation in
1010 plant genomes: Bigger is different. *Am. J. Bot* 105: 16–19. <https://doi.org/10.1002/ajb2.1002>

1011 Nakagawa S., and H. Schielzeth, 2010 Repeatability for Gaussian and non-Gaussian data: a
1012 practical guide for biologists. *Biol. Rev.* 85: 935–956. <https://doi.org/10.1111/j.1469-185X.2010.00141.x>

1013 Neale D. B., and O. Savolainen, 2004 Association genetics of complex traits in conifers.
1014 *Trends Plant Sci.* 9: 325–330. <https://doi.org/10.1016/j.tplants.2004.05.006>

1015 Nowak M. A., M. C. Boerlijst, J. Cooke, and J. M. Smith, 1997 Evolution of genetic
1016 redundancy. *Nature* 388: 167–171. <https://doi.org/10.1038/40618>

1017 O'Connor L. J., A. P. Schoech, F. Hormozdiari, S. Gazal, N. Patterson, *et al.*, 2019 Extreme
1018 Polygenicity of Complex Traits Is Explained by Negative Selection. *Am J hum genet* 105:
1019 456–476. <https://doi.org/10.1016/j.ajhg.2019.07.003>

1020 Orr H. A., and J. A. Coyne, 1992 The Genetics of Adaptation: A Reassessment. *Am Nat* 140:
1021 725–742. <https://doi.org/10.1086/285437>

1022 Pallares L. F., 2019 Searching for solutions to the missing heritability problem. *eLife* 8:
1023 e53018. <https://doi.org/10.7554/eLife.53018>

1024 Palmé A. E., T. Pyhäjärvi, W. Wachowiak, and O. Savolainen, 2009 Selection on Nuclear
1025 Genes in a *Pinus* Phylogeny. *Mol Biol Evol* 26: 893–905.
1026 <https://doi.org/10.1093/molbev/msp010>

1027 Pitchers W., J. Nye, E. J. Márquez, A. Kowalski, I. Dworkin, *et al.*, 2019 A Multivariate

1029 Genome-Wide Association Study of Wing Shape in *Drosophila melanogaster*. *Genetics* 211:
1030 1429–1447. <https://doi.org/10.1534/genetics.118.301342>

1031 Plomion C., J. Bartholomé, L. Bouffier, O. Brendel, H. Cochard, *et al.*, 2016a Understanding
1032 the genetic bases of adaptation to soil water deficit in trees through the examination of water
1033 use efficiency and cavitation resistance: maritime pine as a case study. *JPH* 3: e008.
1034 <https://doi.org/10.20870/jph.2016.e008>

1035 Plomion C., J. Bartholomé, I. Lesur, C. Boury, I. Rodríguez-Quilón, *et al.*, 2016b High-
1036 density SNP assay development for genetic analysis in maritime pine (*Pinus pinaster*). *Mol*
1037 *Ecol Res* 16: 574–587. <https://doi.org/10.1111/1755-0998.12464>

1038 Pritchard J. K., J. K. Pickrell, and G. Coop, 2010 The Genetics of Human Adaptation: Hard
1039 Sweeps, Soft Sweeps, and Polygenic Adaptation. *Curr Biol* 20: R208–R215.
1040 <https://doi.org/10.1016/j.cub.2009.11.055>

1041 Pritchard J. K., and A. D. Rienzo, 2010 Adaptation – not by sweeps alone. *Nat Rev Genet* 11:
1042 665–667. <https://doi.org/10.1038/nrg2880>

1043 R Core Team, 2019 *R: A language and environment for statistical computing*. R Foundation
1044 for Statistical Computing, Vienna, Austria.

1045 Rellstab C., S. Zoller, L. Walthert, I. Lesur, A. R. Pluess, *et al.*, 2016 Signatures of local
1046 adaptation in candidate genes of oaks (*Quercus* spp.) with respect to present and future
1047 climatic conditions. *Mol Ecol* 25: 5907–5924. <https://doi.org/10.1111/mec.13889>

1048 Resende M. D. V., M. F. R. Resende Jr, C. P. Sansaloni, C. D. Petroli, A. A. Missiaggia, *et*
1049 *al.*, 2012 Genomic selection for growth and wood quality in Eucalyptus: capturing the missing
1050 heritability and accelerating breeding for complex traits in forest trees. *New Phytol* 116–128.
1051 <https://doi.org/10.1111/j.1469-8137.2011.04038.x@10.1002>

1052 Robinson G. K., 1991 That BLUP is a Good Thing: The Estimation of Random Effects.
1053 *Statist. Sci.* 6: 15–32. <https://doi.org/10.1214/ss/1177011926>

1054 Rodríguez-Quilón I., L. Santos-del-Blanco, M. J. Serra-Varela, J. Koskela, S. C. González-
1055 Martínez, *et al.*, 2016 Capturing neutral and adaptive genetic diversity for conservation in a
1056 highly structured tree species. *Ecol App* 26: 2254–2266.

1057 Rosenberg N. A., M. D. Edge, J. K. Pritchard, and M. W. Feldman, 2019 Interpreting
1058 polygenic scores, polygenic adaptation, and human phenotypic differences. *Evol. Med. Public*
1059 *Health.* 26–34. <https://doi.org/10.1093/emph/eoy036>

1060 Savolainen O., T. Pyhäjärvi, and T. Knürr, 2007 Gene Flow and Local Adaptation in Trees.
1061 *Ann. Rev. Ecol. Evol. Syst.* 38: 595–619.
1062 <https://doi.org/10.1146/annurev.ecolsys.38.091206.095646>

1063 Savolainen O., M. Lascoux, and J. Merilä, 2013 Ecological genomics of local adaptation. *Nat*
1064 *Rev Genet* 14: 807–820. <https://doi.org/10.1038/nrg3522>

1065 Sefton C. A., K. Montagu, B. J. Atwell, and J. P. Conroy, 2002 Anatomical variation in
1066 juvenile eucalypt leaves accounts for differences in specific leaf area and CO₂ assimilation
1067 rates. *Aust. J. Bot.* 50: 301–310. <https://doi.org/10.1071/bt01059>

1068 Sella G., and N. H. Barton, 2019 Thinking About the Evolution of Complex Traits in the Era
1069 of Genome-Wide Association Studies. *Annu. Rev. Genom. Hum. Genet.* 20: 461–493.
1070 <https://doi.org/10.1146/annurev-genom-083115-022316>

1071 Sharma A., J. S. Lee, C. G. Dang, P. Sudrajad, H. C. Kim, *et al.*, 2015 Stories and Challenges
1072 of Genome Wide Association Studies in Livestock — A Review. *Asian-Australas J Anim Sci*
1073 28: 1371–1379. <https://doi.org/10.5713/ajas.14.0715>

1074 Shi H., G. Kichaev, and B. Pasaniuc, 2016 Contrasting the Genetic Architecture of 30
1075 Complex Traits from Summary Association Data. *Am J hum genet* 99: 139–153.
1076 <https://doi.org/10.1016/j.ajhg.2016.05.013>

1077 Smith J. M., and J. Haigh, 1974 The hitch-hiking effect of a favourable gene. *Genet. Res.* 23:
1078 23–35. <https://doi.org/10.1017/S0016672300014634>

1079 Sohail M., R. M. Maier, A. Ganna, A. Bloemendal, A. R. Martin, *et al.*, 2019 Polygenic
1080 adaptation on height is overestimated due to uncorrected stratification in genome-wide
1081 association studies. *eLife* 8: e39702. <https://doi.org/10.7554/eLife.39702>

1082 Speidel L., M. Forest, S. Shi, and S. R. Myers, 2019 A method for genome-wide genealogy
1083 estimation for thousands of samples. *Nat Genet* 51: 1321–1329.
1084 <https://doi.org/10.1038/s41588-019-0484-x>

1085 Spitze K., 1993 Population Structure in *Daphnia obtusa*: Quantitative Genetic and Allozymic
1086 Variation. *Genetics* 135: 367–374.

1087 Torres-Ruiz J. M., A. Kremer, M. R. Carins-Murphy, T. J. Brodribb, L. J. Lamarque, *et al.*,
1088 2019 Genetic differentiation in functional traits among European sessile oak populations. *Tree*
1089 *Physiol* 39: 1736–1749. <https://doi.org/10.1093/treephys/tpz090>

1090 Turchin M. C., C. W. Chiang, C. D. Palmer, S. Sankararaman, D. Reich, *et al.*, 2012 Evidence
1091 of widespread selection on standing variation in Europe at height-associated SNPs. *Nat Genet*
1092 44: 1015–1019. <https://doi.org/10.1038/ng.2368>

1093 Valladares F., S. Matesanz, F. Guilhaumon, M. B. Araújo, L. Balaguer, *et al.*, 2014 The
1094 effects of phenotypic plasticity and local adaptation on forecasts of species range shifts under
1095 climate change. *Ecol Lett* 17: 1351–1364. <https://doi.org/10.1111/ele.12348>

1096 Visscher P. M., W. G. Hill, and N. R. Wray, 2008 Heritability in the genomics era —
1097 concepts and misconceptions. *Nat Rev Genet* 9: 255–266. <https://doi.org/10.1038/nrg2322>

1098 Visscher P. M., N. R. Wray, Q. Zhang, P. Sklar, M. I. McCarthy, *et al.*, 2017 10 Years of
1099 GWAS Discovery: Biology, Function, and Translation. *Am J hum genet* 101: 5–22.
1100 <https://doi.org/10.1016/j.ajhg.2017.06.005>

1101 Vizcaíno-Palomar N., B. Fady, R. Alía, A. Raffin, S. Mutke, *et al.*, 2019 Patterns of
1102 phenotypic plasticity among populations of three Mediterranean pine species and implications
1103 for evolutionary responses to climate change. *bioRxiv* 716084.
1104 <https://doi.org/10.1101/716084>

1105 Walker X. J., M. C. Mack, and J. F. Johnstone, 2015 Stable carbon isotope analysis reveals
1106 widespread drought stress in boreal black spruce forests. *Glob Chang Biol* 21: 3102–3113.
1107 <https://doi.org/10.1111/gcb.12893>

1108 Warren C. R., J. F. McGrath, and M. A. Adams, 2001 Water availability and carbon isotope
1109 discrimination in conifers. *Oecologia* 127: 476–486. <https://doi.org/10.1007/s004420000609>

1110 Weir B. S., and C. C. Cockerham, 1984 ESTIMATING *F* -STATISTICS FOR THE
1111 ANALYSIS OF POPULATION STRUCTURE. *Evol* 38: 1358–1370.
1112 <https://doi.org/10.1111/j.1558-5646.1984.tb05657.x>

1113 Whitlock M. C., and F. Guillaume, 2009 Testing for Spatially Divergent Selection:
1114 Comparing QST to FST. *Genetics* 183: 1055–1063.
1115 <https://doi.org/10.1534/genetics.108.099812>

1116 Wilson A. J., D. Réale, M. N. Clements, M. M. Morrissey, E. Postma, *et al.*, 2010 An
1117 ecologist's guide to the animal model. *J Anim Ecol* 79: 13–26. <https://doi.org/10.1111/j.1365-2656.2009.01639.x>

1119 Wisser R. J., Z. Fang, J. B. Holland, J. E. C. Teixeira, J. Dougherty, *et al.*, 2019 The Genomic
1120 Basis for Short-Term Evolution of Environmental Adaptation in Maize. *Genetics* 213: 1479–
1121 1494. <https://doi.org/10.1534/genetics.119.302780>

1122 Wray N. R., C. Wijmenga, P. F. Sullivan, J. Yang, and P. M. Visscher, 2018 Common
1123 Disease Is More Complex Than Implied by the Core Gene Omnipotent Model. *Cell* 173:
1124 1573–1580. <https://doi.org/10.1016/j.cell.2018.05.051>

1125 Wright S. I., and P. Andolfatto, 2008 The Impact of Natural Selection on the Genome:
1126 Emerging Patterns in *Drosophila* and *Arabidopsis*. *Ann. Rev. Ecol. Evol. Syst.* 39: 193–213.
1127 <https://doi.org/10.1146/annurev.ecolsys.39.110707.173342>

1128 Yang J., B. Benyamin, B. P. McEvoy, S. Gordon, A. K. Henders, *et al.*, 2010 Common SNPs
1129 explain a large proportion of the heritability for human height. *Nat Genet* 42: 565–569.
1130 <https://doi.org/10.1038/ng.608>

1131 Yeaman S., 2015 Local Adaptation by Alleles of Small Effect. *Am Nat* 186: S74–S89.
1132 <https://doi.org/10.1086/682405>

1133 Young A. I., 2019 Solving the missing heritability problem, (J. Flint, Ed.). *PLoS Genet* 15:
1134 e1008222. <https://doi.org/10.1371/journal.pgen.1008222>

1135 Zeng J., R. de Vlaming, Y. Wu, M. R. Robinson, L. R. Lloyd-Jones, *et al.*, 2018 Signatures of
1136 negative selection in the genetic architecture of human complex traits. *Nat Genet* 50: 746–
1137 753. <https://doi.org/10.1038/s41588-018-0101-4>

1138 Zhang G., L. J. Muglia, R. Chakraborty, J. M. Akey, and S. M. Williams, 2013 Signatures of
1139 natural selection on genetic variants affecting complex human traits. *Appl Transl Genom* 2:
1140 78–94. <https://doi.org/10.1016/j.atg.2013.10.002>

1141 Zonneveld B. J. M., 2012 Conifer genome sizes of 172 species, covering 64 of 67 genera,
1142 range from 8 to 72 picogram. *Nor. J. Bot.* 30: 490–502. <https://doi.org/10.1111/j.1756-1051.2012.01516.x>

Site	Country	Coordinates	Environment	Plantation	N trees	Annual	Summer	Annual mean	Annual	Soil type
						year	(clones)	precipitation	(mm)	temperature
Cabada	Spain	43°25'17" N	Iberian	2010	4,272	890	126	12.9	24.0	Cambisol
		06°32'38" W	Atlantic		(535)					
Fundão	Portugal	40°06'38" N		2010	4,272	1122	58	14.0	26.9	Cambisol
		07°28'58" W			(535)					
Pierrotin	France	44°44'42" N	French	2011	3,434	933	199	13.8	26.7	Arenosol
		00°47'04" W	Atlantic		(443)					
Madrid	Spain	40°30'47" N	Mediterranean	2010	4,272	378	35	14.8	32.8	Arenosol
		03°18'44" W			(535)					
Cáceres	Spain	40°02'24" N		2010	4,272	374	21	16.7	32.6	Fluvisol
		05°22'19" W			(535)					

Table 1. CLONAPIN common garden network (5 sites). Climatic data correspond to the mean of each parameter for the period 2005-2014 obtained from the EuMedClim database (Fréjaville and Benito Garzón 2018).

Trait	Environment	Gene set	Statistic tested	Sign of enrichment	p-value	q-value (<0.10)
Height	French Atlantic	<i>Transcription factor</i>	<i>maxabsbetarb</i>	Higher	0.003	0.05
			<i>maxpostprb</i>	Higher	0.004	0.07
	Mediterranean	<i>Cytoskeleton</i>	<i>maxabsbetarb</i>	Lower	0.003	0.06
Survival	Iberian Atlantic	<i>Transcription factor</i>	<i>maxabsbetarb</i>	Higher	0.001	0.01
			<i>maxpostprb</i>	Higher	<0.001	0.005
Bud burst 2015	French Atlantic	<i>Monolignol biosynthesis</i>	<i>maxabsbetarb</i>	Higher	0.003	0.05
		<i>Monolignol biosynthesis</i>	<i>maxpostprb</i>	Higher	0.005	0.08
		<i>Glycan metabolism</i>	<i>maxabsbetarb</i>	Lower	0.040	0.09
Phenology growth index	Iberian Atlantic	<i>Cell growth and death</i>	<i>maxabsbetarb</i>	Lower	0.010	0.03
		<i>DNA recomb and repair</i>	<i>maxabsbetarb</i>	Lower	0.008	0.03
		<i>UV response</i>	<i>maxabsbetarb</i>	Lower	0.005	0.03
<i>D. sapinea</i> necrosis	French Atlantic	<i>Ubiquitin system</i>	<i>maxabsbetarb</i>	Higher	0.002	0.04
			<i>maxpostprb</i>	Higher	0.003	0.06
<i>D. sapinea</i> discoloration	French Atlantic	<i>Signal transduction</i>	<i>maxabsbetarb</i>	Higher	0.004	0.08
			<i>maxpostprb</i>	Higher	0.003	0.06
		<i>Flavonoid biosynthesis</i>	<i>maxpostprb</i>	Higher	0.007	0.07

Table 2. Gene sets with gene function enrichment at pathway/module level. Two statistics obtained from the VSR method were tested: the maximum of any SNP per gene of the Rao-Backwellized posterior probability of inclusion (*maxpostprb*) and the maximum of any SNP per gene of the absolute value of the Rao-Backwellized effect-size (*maxabsbetarb*). Sign of enrichment refers to two-tailed null hypothesis testing.

Figures

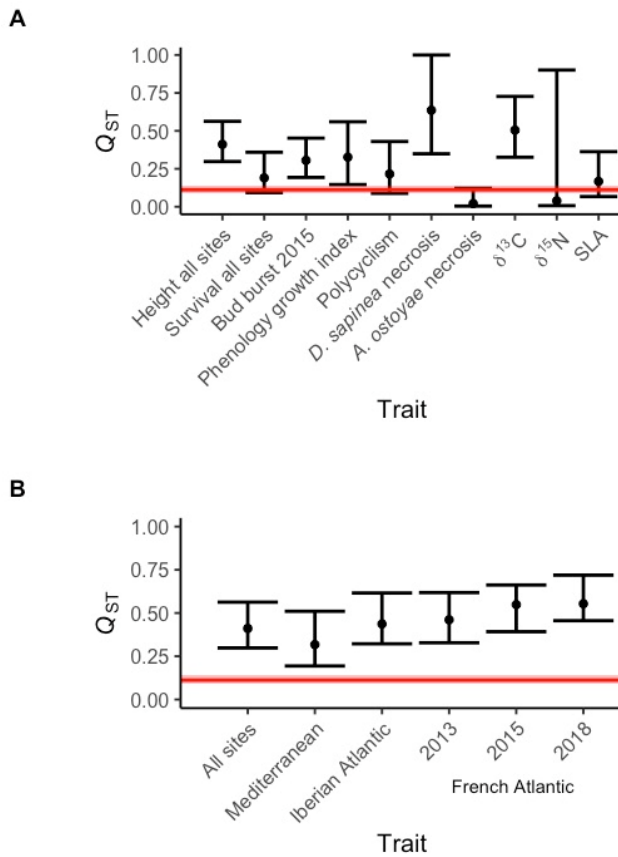


Figure 1. Comparison of Q_{ST} and F_{ST} estimates across traits, environments and years. A) Q_{ST} for a selection of traits belonging to five categories: survival, height, phenology-related traits, functional traits and biotic-stress response (see Supplemental Table S1 for all traits). B) Q_{ST} for height estimated in three different environments: Mediterranean, Iberian Atlantic, and French Atlantic, and a global Q_{ST} for the three environments together. In the French Atlantic common garden, height was measured in three different years: 2013, 2015 and 2018. Global F_{ST} estimate is presented by a red line surrounded by the 95% confidence intervals computed by bootstrapping.

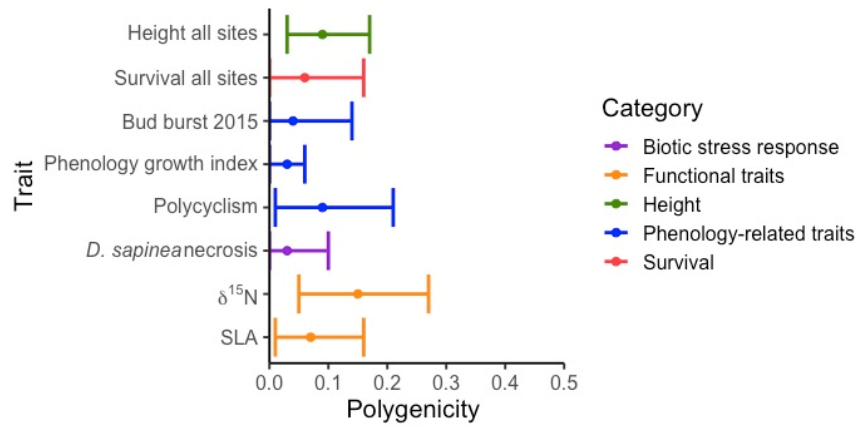


Figure 2. Polygenicity estimated from Bayesian mixed linear models (MLMs) for a selection of traits (see Supplemental Table S4 for all traits). Polygenicity was estimated as the proportion of non-zero size-effect SNPs. Posterior median and 95% credible intervals are presented.

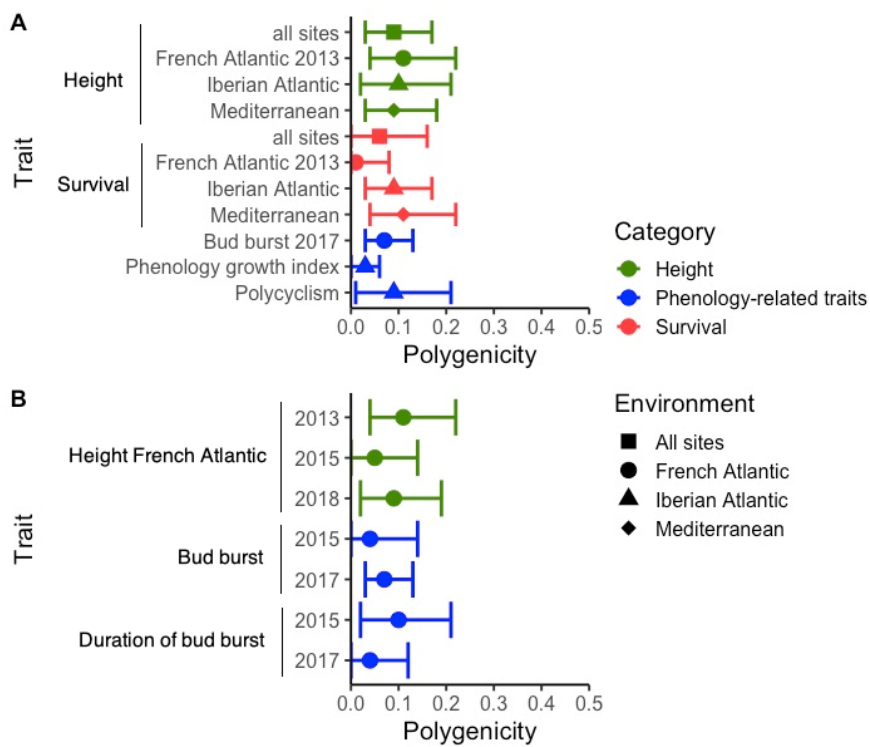


Figure 3. Polygenicity estimated from Bayesian mixed linear models (MLMs) across environments and years. A) Variation of polygenicity across environments. B) Temporal variation of polygenicity. Polygenicity was estimated as the proportion of non-zero size-effect SNPs. Posterior median and 95% credible intervals are presented.

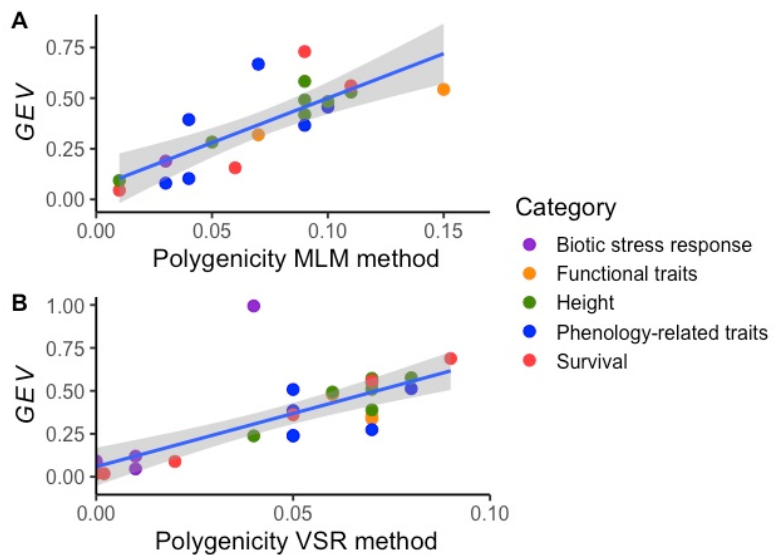


Figure 4. Correlation between polygenicity (proportion of non-zero size-effect SNPs) and GEV (explained genetic variance). A) MLM method implemented in CGTB software. B) VSR method implemented in piMASS software. Each point represents the posterior median.

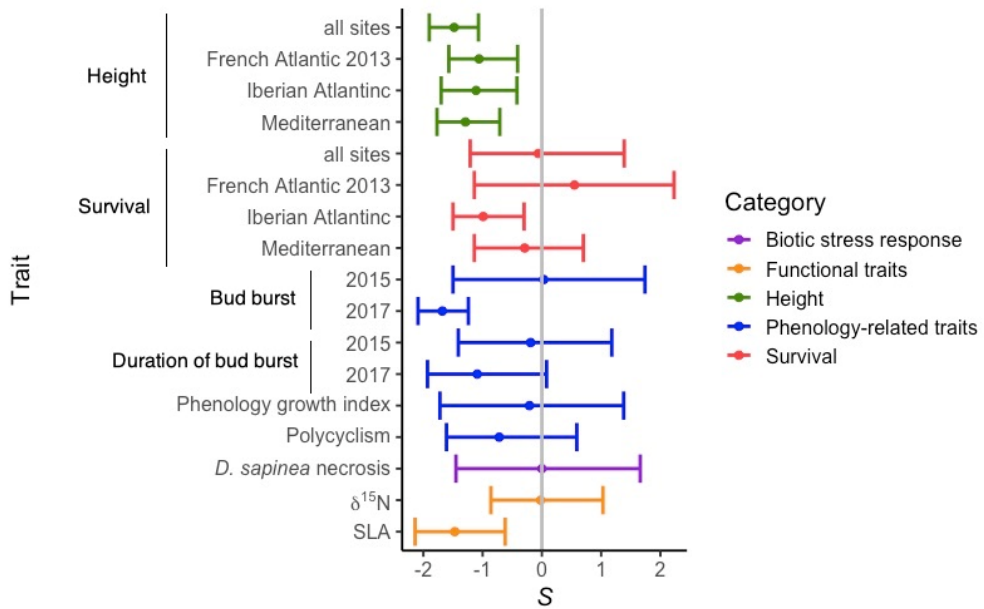


Figure 5. Correlation between SNP effect-size and Minor Allele Frequency (MAF). The coefficient of correlation between SNP effect-size and MAF (S) was estimated through the MLM method. The posterior distribution of S (median and 95% credible intervals) are presented.